CHAMP and SAC-C Atmospheric Occultation Results and Intercomparisons

G. A. Hajj[1], C. O. Ao[1], B. A. Iijima[1], D. Kuang[1], E. R. Kursinski[1,2], A. J. Mannucci[1], T. K. Meehan[1], L. J. Romans[1], M. de la Torre Juarez[1], T. P. Yunck[1]

(1) Jet Propulsion Laboratory, California Institute of Technology
(2) University of Arizona, Department of Atmospheric Sciences

(submitted to JGR-Atmosphere, August 2, 2002)

Abstract

The German CHAMP (CHAllenging Minisatellite Payload) and Argentine SAC-C (Satelite de Aplicaciones Cientificas-C) Earth science missions, launched in 2000, carry a new generation of Global Positioning System (GPS) receivers for radio occultation sounding of the ionosphere and neutral atmosphere. Though the occultation concept for obtaining profiles of atmospheric temperature, pressure and moisture was proven in 1995with GPS/MET, concurrent measurements from CHAMP and SAC-C present the first opportunity to test three central claims: (1) GPS soundings are effectively free of instrumental bias and drift; (2) individual temperature profiles are accurate to <0.5K between ~5-20 km; and (3) averaged profiles for climate studies can be accurate to <0.1K. These properties imply that a weak climate signal can be detected in less than a decade and studied by different instruments at different times with no external calibration. In this paper these claims are attested by comparing nearby CHAMP and SAC-C profiles. Of 60,000 profiles examined, 60 pairs occurring within 30 min and 200 km of one another were found. Profiles pairs agree to <0.5K (68% confidence interval) and to within 0.1K in the mean between 5-20km altitude, after removing the expected variability of the atmosphere. Individual comparisons show closest agreement near the tropopause, and display finer resolution and substantially different temperatures than numerical weather model analyses from the National Center for Environmental Prediction (NCEP) and the European Center for Medium-Weather Forecast (ECMWF). The inferred error on the analyses is 1-1.5K. Comparisons between CHAMP and SAC-C largely indicate precision; however, several features observed in common, especially near the tropopause, tend also to indicate accuracy. Limitations of previous experiments (e.g., GPS/MET) in probing the lower troposphere are largely overcome with CHAMP and SAC-C, with the majority of profiles (60%) descending to the lowest 0.5 km. This is expected to increase to 90-95% with future system improvements. Examples are selected to illustrate lower-tropospheric sensing, including detection of the planetary boundary layer top with a vertical resolution of ~100 m. For the first time, such performance is achieved with GPS Antispoofing encryption on. Daily occultations currently number ~350; this is expected to reach over 1000 in the next year, rivaling the number of semi-daily radiosonde launches. With several new missions in planning this may increase ten-fold in the next 3-8 years, making GPS sounding a vital input to numerical weather prediction and climate research.

1. Introduction

The concept of atmospheric profiling by GPS occultations was first introduced in 1988 [Yunck et al.; 1988] and later demonstrated with the GPS/MET experiment in 1995 [Ware et al., 1996]. The concept is derived from planetary occultation experiments where measurements of signal time delay of a spacecraft occulted behind a planet as viewed from Earth is used to infer properties of the planet's atmosphere [e.g., Fjeldbo et al., 1971]. Applied to Earth, the transmitter is a GPS satellite and the receiver is placed on a low-Earth orbit (LEO). The fundamental measurement is the time delay of the transmitted GPS signal as the satellite sets or rises behind Earth's atmosphere. Precise time delay measurements are converted into atmospheric Doppler shift and bending, from

which atmospheric refractivity, density, temperature, pressure and water vapor can be inferred.

After the successful demonstration of this concept with the GPS/MET experiment in 1995 [e.g., Ware et al., 1996; Hajj et al., 1996; Kursinski et al., 1996; Leroy, 1997; Rocken et al., 1997; Kursinski and Hajj, 2001], several challenges remained:
(1) Obtaining accurate retrievals when the GPS signal is encrypted (referred to as Anti-spoofing or AS) by the Department of Defense (DoD)[1].
(2) Obtaining a sufficient density of occultations to facilitate scientific and operational use of the data.
(3) Penetrating the lower troposphere in moist regions.
(4) Demonstrating sub-Kelvin temperature accuracy.

Overcoming these challenges is crucial to meeting the full potential of GPS occultation science; applications which include improving our understanding of the planetary boundary layer (PBL), troposphere-stratosphere exchange, water vapor circulation, heat and energy transport by gravity waves, climate monitoring and fingerprinting, and weather prediction. GPS occultations promise to provide global atmospheric profiling with high vertical resolution (0.1-1km) and high accuracy (< 1K temperature, < 0.5 g/kg specific humidity) under all weather conditions. Moreover, because GPS occultation is an active measurement, it yields an independent estimate of pressure as a function height, therefore, enabling the determination of geopotential heights with an accuracy reaching1-2 m. The geopotential height of a pressure level is a measure of the atmospheric weight above it and can be used as a sensitive gauge of climate trends.

The launch of the German CHAMP (CHAllenging Minisatellite Payload) and the Argentine SAC-C (Satelite de Aplicaciones Cientificas-C) missions in 2000, carrying a new generation of GPS receivers, enables us to address the challenges listed above. In this paper we describe these four challenges and demonstrate that the current missions have, for the most part, solved them. The first challenge is solved by use of a new generation "semi-codeless" GPS receiver which enables accurate tracking of the GPS signals while AS is turned on. The second challenge is met as both missions continuously provide 400+ occultations every day, a number that will soon reach 1000+ to match the daily number of radiosonde profiles that form a crucial input to weather prediction models.

In comparison with the earlier GPS/MET instrument, these new receivers substantially improve our ability to sense the lower troposphere. Here we present result demonstrating consistent penetration down to the lowest kilometer of the atmosphere for most of the CHAMP and SAC-C occultations. With routine sensing of the lower troposphere, GPS occultations provide the first remote sensing technique that is able to sense the PBL and the transition into the free troposphere with a high vertical resolution.

[1] AS on is the normal mode of operation for GPS. During the GPS/MET experiments in 1995-1997, AS was turned off for 4 three-week periods for the sake of demonstrating GPS profiling.

A substantial part of this paper is devoted to addressing the fourth challenge, to demonstrate sub-Kelvin accuracy. This challenge can be broken into three central claims:
(a) GPS occultation profiles are free of instrumental drift and are virtually unbiased;
(b) Individual GPS temperature retrievals have 0.5K accuracy between ~5-25 km and approach 0.2 K accuracy near the tropopause;
(c) Averaged profiles for use in climate studies can reach a temperature accuracy of 0.1 K or better at these altitudes.

The first implies that temperature measurements obtained today from GPS occultations can be compared to temperature measurements obtained from GPS occultations a decade later (with the same or different receiver) without concern for instrumental drift or calibration. Because the measurements are both precise and virtually absolute, small changes in average temperature over this period can be detected. If claims (b) and (c) can be verified, they would establish GPS occultation as the most accurate spaceborne technique for measuring tropospheric and stratospheric temperatures and for detecting subtle climate trends.

The difficulty in testing these claims stems from the lack of current measurements or models more accurate than about 1K, making comparisons with other data sources of limited value. Such comparisons have been performed by numerous groups (see e.g., Kursinski et al., [1996] or Rocken et al., [1997] for GPS/MET; Wickert et al., [2001] or Hajj et al., [2002a] for CHAMP) and have established that GPS temperatures are consistent with those of radiosondes, satellite radiometers and weather forecasts to about 1-2K between 5-25km. While such comparisons are valuable, they cannot tell us which of the compared quantities is more accurate. And while detailed theoretical analysis (e.g., Kursinski et al., 1997) suggests GPS soundings to be accurate to better than 0.5 K between 5-25 K and about 0.2 K at the tropopause, this has not yet been demonstrated. The presence now of two sensors taking GPS measurements independently from different vantage points provides our first opportunity to test such claims rigorously and to establish better precision and accuracy estimates for current GPS retrievals.

We should stress that these claims of precision and accuracy are valid only in regions where effects of water vapor on the occulted signal can be ignored. Since the saturation water vapor pressure decreases rapidly with decreasing temperature, as dictated by the Clausius-Lapeyron equation, water vapor in tropospheric regions where $T < 250$ K can be ignored [Kursinski et al., 1995], and sub-Kelvin accuracy in these regions is expected. This condition extends down to the surface near the pole, making this technique promising for detecting climate variation at the Arctic and Antarctic regions.

In regions where water vapor becomes significant, accuracy claims can be translated in terms of refractivity (N) to 2 parts in 1000 from the surface to 30 km. Early validation of refractivity against weather analyses has shown a negative bias in the lower troposphere. This was attributed to the GPS occultations by Rocken et al. [1997] and to the weather analyses by Kursinski and Hajj [2001]. The truth is most likely somewhere in the middle. A number of factors can cause the GPS occultation refractivity to be negatively

biased in a moist region, including the momentary disappearance of the occulted signal due to total internal reflection [Sokolovskiy, 2000] and systematic deviations from spherical symmetry assumed by the Abel transform, which is the basis of all current GPS occultation retrievals. A full treatment of the refractivity bias (or N-bias) would require a separate study; suffice to say that the sources of this bias are being aggressively pursued at JPL and elsewhere and, to the extent it arises within the occultations, we can expect it soon to be understood and eliminated. Meanwhile, we shall limit our validation efforts to temperatures derived in dry regions, where $T < 250$ K or in the stratosphere.

Occultations from CHAMP and SAC-C have been collected since the middle of 2001. To date, the two missions have gathered $\sim 10^5$ occultations. To keep up with the stream of occultation data, a versatile data analysis system is set up at the Jet Propulsion Laboratory (JPL), allowing us to process and examine the data continuously. Our presentation starts with an overview of this occultation processing system (section 2).

A prerequisite to obtaining high-quality retrievals is the computation of precise orbits of the GPS and the LEO satellites. Accuracies of CHAMP and SAC-C orbits are examined in section 3. In sections 4-7 we address, in order, challenges 1-4 listed above. In section 4 we examine the signal noise properties and how they map into retrieved temperature errors. We also perform statistical comparisons to weather analyses to assess current retrieval accuracy with AS on compared to that of GPS/MET with AS off. In section 5, we examine the number of daily occultations collected by both missions and their coverage. Section 6 addresses current performance in sensing the lower troposphere. This is done by showing specific examples where the PBL is detected and by statistical analysis to assess the degree of success in penetrating the lower troposphere. In section 7 we directly compare CHAMP and SAC-C occultations, presenting individual examples and statistics. Conclusions are summarized in section 8.

2. An Overview of the JPL Occultation Processing System

The occultation data analysis system at JPL consists of a number of processes which can be grouped under four main categories (Figure 1):

Figure 1

(1) Data collection: In this process, flight and ground data are collected, reformatted, corrected for bit errors and flagged for cycle slips. Ground data consists of two types, medium-rate data collected at 1 Hz, and low-rate data collected at 1/30 Hz. The former is used for GPS-occultation calibration in which the GPS clocks are solved for at the 1-second rate and removed. (The demise of GPS clock dithering—known as selective availability—has made it possible to use low-rate ground data for GPS-occultation calibration; see Wickert et al., 2002). The latter is used to solve for the GPS orbits.

(2) Orbit determination: Both GPS and LEO orbits are needed for the processing of occultation data. Three types of GPS daily orbit solutions are routinely generated at JPL with different production speed and accuracy: (1) The "FLINN" final orbits, produced about 1 week after the fact, with an orbit accuracy of ~5 cm; (2) "QuickLook" orbits, produced daily, with an accuracy of ~15 cm; and (3) continuous real-time orbits accurate to ~0.25 m. Our current occultation processing adopts the

QuickLook orbits, allowing us to produce retrievals within 24 hrs of data collection. For use in numerical weather prediction, where <3 hrs of delay is required, one could adopt the real-time GPS orbits with little performance penalty. In that case the latency will depend largely on the downlink time of the LEO data.

(3) Calibration process: In the calibration process, the atmospheric delay induced on the occulted link is isolated by removing all clock drifts and the geometric delay change due to the motion of the satellites. Our normal processing system uses four links, LEO-GPS1, LEO-GPS2, Ground-GPS1 and Ground-GPS2 in a double-differencing geometry to solve for and remove all clock errors. The technique is widely used in geodesy. Its application to GPS occultation is described in detail in Hajj et al., 2002b. More recently, it has been shown that with SA turned off, a single difference (LEO-GPS1 minus LEO-GPS2) is sufficient for accurate temperature retrievals [Wickert et al., 2001]. Since further assessment of single differencing is still needed to establish its true performance, our routine analysis still employs double differencing.

(4) Retrieval process: At this point, the atmosphere-induced Doppler and bending are derived, the ionosphere is removed by taking a linear combination of the L1 and L2 bending at the same impact parameter and the Abel inversion is performed on the calibrated bending to derive refractivity. Once refractivity is obtained, the hydrostatic integral is initialized by using the temperature at 30 km altitude from the National Center for Environmental Prediction (NCEP) final analysis. Similarly because of the "moist-dry" ambiguity in interpreting the refractivity in the lower-troposphere, the NCEP temperature is used in the lower-troposphere at levels where $T > 250K$ in order to derive water vapor pressure from the GPS occultations. The detail of the processing is described in [Hajj et al., 2002b]. Finally, a quality control check is applied to the final product. An occultation is considered successful only if its temperature difference from the NCEP analysis is less than 10 K and its fractional refractivity difference to NCEP is less than 20% everywhere below 30 km.

A key element of the occultation analysis system is an automated *executive* which triggers each process upon completion of the previous one. Once the data are downlinked from the satellite and transferred to JPL, the executive fetches the required GPS orbits and triggers the LEO-orbit process. Completion of the LEO orbit then triggers calibration followed by retrieval. These processes can run on different machines and for different occultations simultaneously allowing maximum flexibility, speed, and autonomy.

3. CHAMP and SAC-C Orbits

Since the fundamental measurement during an occultation is the time delay between the transmitted and received signal, obtaining accurate orbits is necessary to remove orbital motion effects and isolate the atmospheric delay. The precision and accuracy of the orbits also indicate the health of the receiver in general and the quality of the data used in doing precise orbit determination (POD). In this section we discuss the precision and accuracy of our orbital solutions for CHAMP and SAC-C.

The orbits of both CHAMP and SAC-C are determined using the GPS measurements collected by a zenith-looking antenna. Both the zenith-looking and the aft-looking (used

for occultations) antennas are connected to the same GPS receiver. Because of the low altitudes of the SAC-C (710 km) and CHAMP (410 km) satellites operating close to solar-maximum conditions, their motions are subject to sizable geopotential and atmospheric drag perturbations. The orbit determination task would require precise modeling of these perturbations if it relied on a purely dynamical approach. At JPL we apply a reduced-dynamic strategy in which local stochastic accelerations are adjusted to compensate for mis-modeled forces. By tightening or loosening the constraint on the stochastic accelerations, we can tune the reduced-dynamic orbit solution to optimize between dynamic and kinematic solutions [Yunck et al., 1990, Wu et al., 1991, Bertiger et al., 1994]. In order to obtain an optimal combination of the geometric information in the measurements and the knowledge in the orbit dynamic models, different constraints were selected for CHAMP and SAC-C through separate tuning processes similar to those discussed by Kuang et al., [2001].

In solving for CHAMP and SAC-C orbits, the GPS satellite orbits and their clock solutions (produced daily at JPL based on data from the International GPS Service ground receiver network) are used. For each day, we process 27 hour of flight tracking data (24 hrs + 3 hrs from previous day) and take the last 26 hours arc as the precise orbit solution. Orbit precision is evaluated using the differences in the 2 hours of overlapping period between two consecutive 26-hour orbit solutions. The orbit overlap difference is a self-consistency test, measuring orbit precision not accuracy. However, past experience [e.g., Bertiger et al., 1994] has suggested that orbit overlap difference can be a good approximation of orbit accuracy if we use it with caution and use other tests to detect possible systematic errors. Figure 2 shows the overlap difference RMS for CHAMP orbit position and velocity during a 9 day period (June 1 – June 9, 2002). Figure 3 shows the orbital overlap difference RMS for SAC-C for the same period. Both CHAMP and SAC-C show a RMS overlap differences of < 8 cm for position and < 0.05 mm/sec for velocity in the radial, cross-track and along-track directions. Of most importance to occultation measurements is the velocity along-track component which shows a consistency of < 0.08 mm/sec for all days, meeting or exceeding the velocity accuracy requirements for GPS occultations at the altitudes of consideration here (< 50 km) [Melbourne et al., 1994; Kursinski et al., 1997].

Figure 2

Figure 3

A measure of the CHAMP orbit accuracy is possible by use of the laser reflector on CHAMP and Satellite Laser Ranging (SLR) data taken from a global network of ground stations. Table 1 shows the RMS and standard deviation of SLR range residuals available during the 9 day period mentioned above. Each residual is the difference between the SLR measured range and the computed range using our CHAMP orbit solution. All residuals shown here are derived from raw SLR measurements without any correction to time tag biases. . The average RMS value of these SLR residuals is 7 cm, verifying that the orbit overlap difference serves as a reasonably good orbit accuracy evaluation in this case.

Table 1

4.0 Assessment of CHAMP and SAC-C Performance

A basic condition for the success of GPS/MET was the temporary disabling of the DoD anti-spoofing in which the second (L2) GPS signal is encrypted. The new generation "Blackjack" receiver on board CHAMP and SAC-C has an advanced "semi-codeless" capability which allows the recording of accurate L2 even when AS is on. In this section, we examine the fundamental observables (phase and amplitude of the occulted signal) recorded by CHAMP and SAC-C and perform statistical comparison of retrieved refractivity, temperature and specific humidity to the NCEP weather analysis.

4.1 Evaluation of basic observables

The fundamental measurements during an occultation are (a) the phase delay, which is a measure of the travel time between the occulted transmitter and receiver pair up to an unknown constant, and (b) the voltage signal-to-noise ratio (SNR) of the occulted signal, reflecting the received signal amplitude. Various techniques have been introduced in which phase [Fjedbo et al., 1971], amplitude [e.g., Sokolovskiy, 2000] or a combination of both [e.g., Melbourne et al, 1994; Gorbunov et al., 1996; Karayel and Hinson, 1997; Gorbunov et al., 2000] measurements are used to derive profiles of atmospheric refractivity. Here we examine both types of measurements for CHAMP and SAC-C.

Voltage Signal to Noise Ratio (SNR)

Because of the inverse relationship between phase noise and SNR ($\sigma_\phi = SNR^{-1}$), an occultation with higher SNR translates into a more accurate refractivity retrieval. Below we examine the average SNR for CHAMP and SAC-C for the two GPS frequencies (L1@19.0 and L2@24.4 cm) and how they compare to the GPS/MET experiment. Figure 4 shows the average SNRs over one full day of CHAMP, SAC-C, and GPS/MET occultations for both L1 and L2. For GPS/MET, averages from two different periods are shown, corresponding to times when AS was both off and on. The overall decay of the SNR as a function of time for all satellites is due to defocusing of the occulted signal as it experiences more bending in the lower part of the atmosphere. However, by comparing the "free space" SNR at the beginning of the occultations, we notice that CHAMP and SAC-C have considerably higher SNR than GPS/MET. In the case of the L1 signal, this is mainly due to the 10 dB and 9 dB receiving antenna gains for CHAMP and SAC-C, versus the 6 dB maximum gain on GPS/MET. However, for L2, the substantial improvement in CHAMP and SAC-C L2 (collected with AS on), over the AS-on GPS/MET L2, is due to the advanced semi-codeless tracking by the BlackJack receivers on CHAMP and SAC-C. This improvement in L2 SNR is crucial for obtaining high-accuracy retrievals with an unclassified receiver. By contrast, during AS-on periods, the low GPS/MET L2 SNR (Figure 4) caused L2 phase measurements to be noisier and, in many cases, impossible to track, precluding dual-frequency retrievals nearly 88% of the time [2].

Figure 4

[2] To overcome this limitation in GPS/MET, a single frequency retrieval scheme, at the expense of lower accuracy and resolution, was introduced to process AS-on GPS/MET periods [de la Torre et al., 2002].

Phase Measurements

An example of phase measurements from a CHAMP occultation (after removing clocks and orbital motion) is shown in Figure 5 (left scale). We note that the 2.5 km extra atmospheric delay, contrasted with the 1-1.5 km delay observed in GPS/MET, is an indication of the deeper penetration of the occultation in the lower troposphere for CHAMP and SAC-C. We examine the noise of the phase measurements by differentiating the atmospheric delay twice with respect to time. The results are shown on the right scale of Figure 5. The significantly noisier Doppler rate toward the latter part of the occultation corresponds to when the signal is in the lower troposphere and is a result of a decreasing SNR. On the other hand, in the first half of the occultation, a most notable feature is a periodic signal at 1Hz rate. This is due to the non-perfect cancellation of the receiver's clock when forming the difference between the occulted and the non-occulted reference signals. This effect is more adverse for CHAMP and SAC-C than it was for GPS/MET and is due to some hardware and software implementation that are specific to CHAMP and SAC-C. Several fixes are in progress to eliminate this; for the time being, we need to understand the implication of having such periodic noise on the retrievals.

Figure 5

To quantify the effect of the 1Hz signal on the retrieval, we process the occultation of Figure 5 as follows: (a) smooth the phase with a 2-sec smoothing window; (b) construct a noisy phase by adding an error of +1.5 cm (corresponding to the averaged observed error) at 0.02 seconds before and -1.5 cm at 0.02 seconds after each 1-sec mark of the smoothed phase; (c) retrieve the artificially constructed phase by use of three different smoothing windows and sampling times: (1) a 1-second smoothing window sampled at 1Hz rate, (2) a 1-second smoothing window sampled at 3 Hz and (3) a variable smoothing window commensurate with the time it takes the occulted link to cross a Fresnel's diameter size sampled at 3 Hz. Figure 6 shows the difference in the retrieved refractivity and temperature between the smoothed and noisy phase measurements (obtained in steps (a) and (b), respectively) for the three different smoothing schemes. With this procedure, and by use of the second retrieval scheme (1-sec smoothing window sampled at 3 Hz), we estimate that the contribution of the 1Hz noise to temperature error is <0.2K below 30 km and <0.1K below 25 km. We shall see that these errors are well below the expected errors on CHAMP and SAC/C temperature profiles at these heights, and therefore, adopt the second retrieval scheme as our main approach to processing the data.

Figure 6

4.2 Statistical Comparisons to Weather Analysis

A standard method of assessing the quality of GPS occultation retrievals has been to compare them against weather analyses. Figure 7 shows means and standard deviations of fractional refractivity, temperature and specific humidity differences between profiles obtained by GPS occultations and corresponding profiles obtained from semi-daily final NCEP analysis interpolated to the locations and times of the occultations. Two sets of statistics are shown, one for CHAMP and one for SAC-C, computed based on data from

Figure 7

June 1-7, 2002 (coverage shown in Figure 9). The following features are worthwhile noting: (1) Both satellites show remarkably similar statistics when compared to the analysis. This is an indication of the consistency between CHAMP and SAC-C measurements and can be used as an indication of the precision of these measurements although a more thorough treatment is given later (section 7). (2) Temperatures are consistent with the analysis to < 0.5K in the mean and 1-2K in standard deviation. These ranges are similar to what was observed with GPS/MET data during AS-off periods [Kursinski et al., 1996; Rocken et al., 1997]. Therefore, the performance of CHAMP and SAC-C with AS on at least equals that of GPS/MET with AS off. By contrast, statistics from GPS/MET and Oersted for data collected during AS-on periods show differences with standard deviation of order 2-4 K [de la Torre et al., 2002]. (3) On average, CHAMP and SAC-C refractivities are smaller than the analysis by ~1-2% in the lower troposphere resulting in a ~0.5 g/kg smaller specific humidity. This bias has been attributed to the occultations by Rocken et al. [1997] and to the model by Kursinski and Hajj [2001]. A more detailed analysis of the origin of this bias is needed and will be deferred to a future study.

5. Number of Daily Occultations and Coverage

A dense coverage of daily occultations and their processing in a timely manner are necessary if this type of data is to become useful for scientific and operational use. The presence of CHAMP, which carries an aft-viewing antenna, and SAC-C, which carries both fore and aft antennas, would, in principle, provide nearly 750+ occultations (250 from each antenna). In addition, the recent launch of the Gravity Recovery and Climate Experiment (GRACE) mission, also with a fore and aft antennas, will add 500 more daily soundings, bringing the total to ~1250 profiles/day. This surpasses the number of semi-daily radiosonde launches, which form a crucial input for weather analysis, and provides new data in remote areas lacking radiosonde coverage. Several operational missions are planned during the next 3-10 years, including the Constellation Observing System for Meteorology, Ionosphere and Climate (COSMIC, 6 satellites), Atmospheric Climate Experiment (ACE+, 4 satellites), National Polar-orbiting Operational Environmental Satellite System (NPOESS, 3 satellites), the European Operational Meteorology (MetOp) satellites, in addition to several missions of opportunity, bringing the potential daily total of GPS soundings to several thousands.

Because the forward viewing antenna on SAC-C is not yet enabled, the current target number of daily occultations is 500. Figure 8 shows the number of weekly occultations collected and processed at JPL for CHAMP and SAC/C. For an occultation to be considered successful it must pass three key processing steps: (1) calibration, where the atmospheric delay induced on the occultation link is isolated, (2) retrieval, where the delay is converted into atmospheric parameters, and (3) quality control, where key solution parameters are checked to be within reasonable physical bounds. Figure 8 shows the number of weekly occultations failing calibration (red), retrieval (yellow), and quality control (blue), and the number passing all three steps (green). We note that the yield (number of successful occultations) has increased over time for both missions. This is due to various receiver software upgrades and improvements to the analysis system

Figure 8

described in section 2. Over the last weeks shown in Figure 8, the average number of successful daily occultations from both satellites is ~350.

A principal source of failure is in the calibration process due to one or more missing links required in double differencing [Hajj et al., 2002b]. The majority of these failures are due to missing LEO-to-reference GPS satellites used to remove LEO clock errors. Other causes of failure include noise in the retrievals at high (>30 km) and low (<5 km) altitudes which cause the occultation to fail the retrieval step and/or the quality control test. The quality control test merely checks the temperature difference between the occultation and NCEP is <10 deg below ~30 km and the refractivity fractional difference is < 20% below ~30 km. While this rather simple test might remove some good profiles where the analyses are in error, and pass others with sizable errors, it is sufficiently robust to eliminate obvious outliers among the occultations.

An example of the coverage from CHAMP and SAC-C for the week of June 1-7, 2002 is shown in Figure 9. The global nature of the measurements is evident with a lower density in the tropics than at high latitude. This is due to the high-inclination of CHAMP and SAC-C and their viewing geometry relative to GPS. A LEO at low-inclination (<30 deg) would significantly improve the coverage near the equator[3].

Figure 9

6. Sensing the Lower Troposphere

Due to signal defocusing and high signal dynamics introduced by sharp structures in the lower troposphere, tracking the occulted GPS signal in that region has proven to be difficult. For example, our experience with GPS/MET has shown that very often the GPS signal is lost in the lower troposphere in regions of high water vapor concentration. An exception was a period during June-July of 1995 where the signal penetrated to the lowest 2 km in the majority of cases [Kursinski and Hajj, 2001]. That improvement resulted from an experimental mode of operation in the receiver known as "fly-wheeling." That same mode, with some enhancements, is on CHAMP and SAC-C, allowing profiles to penetrate the lowest 0.5 km of the atmosphere in the majority of cases.

The left panel of Figure 10 shows the percentage of occultations that reach below a certain height for CHAMP (a similar value is obtained for SAC-C) at different latitude bands. The figure also shows the penetration of occultations from the GPS/MET fly-wheeling period (middle panel) and a GPS/MET period with no fly-wheeling (right panel). We see that penetration into the lowest ½ km over the entire globe has gone from ~5% (no fly-wheeling) to 30% (GPS/MET fly-wheeling) to ~60% for CHAMP. Further improvement is expected with the implementation of 'open-loop' tracking on CHAMP and SAC-C.

Figure 10

[3] The first low-inclination satellite with GPS occultation capability will be C/NOFS (Commncations/Navagation Outage Forecasting System) which is scheduled for launch in 2005 at 12 deg. inclination mainly for ionospheric sensing.

A number of issues complicate tracking in the troposphere. We can illustrate these with an occultation acquired by CHAMP on 1 Oct 2001. We start by examining the SNR for this occultation (Figure 11) which shows a disappearance of the signal at 40 sec into the occultation and then its reappearance nearly 8 seconds later for a few seconds before it finally disappears. This temporary "blocking" of the signal is caused by atmospheric ducting or strong super refraction when the tangent height of the signal is immediately below the inversion height of the PBL. The corresponding temperature and partial water vapor pressure (WVP) profiles obtained from this occultation are shown in Figure 12, along with NCEP analysis and other measurements from nearby radiosondes. The WVP is obtained by assuming the NCEP temperature. The profiles are obtained by use of the canonical transform approach [Gorbunov*,* 2001] which maintains the highest possible vertical resolution and overcomes some difficulties associated with atmospheric multipath.

Figure 11

Figure 12

The PBL top in Figure 12 is seen clearly in the WVP structure at ~1.8 km with a sharp transition in moisture content between the boundary layer and free troposphere. This sharp gradient of refractivity intensifies atmospheric effects and can cause total internal reflection resulting in signal disappearance, providing an extremely accurate location of the inversion height. Thus the signal disappearance, far from being purely a liability, can provide valuable and extremely precise information about atmospheric structure. By contrast, the NCEP analysis displays a smoother transition relative to the CHAMP and radiosonde data. This indicates a lack of vertical resolution and of dynamics in the model needed to create a sharp transition at the inversion height. Although atmospheric ducting on GPS occultation was first observed and successfully modeled with measurements taken atop Mauna Kea in Hawaii [Hajj et al*.,* 1994], CHAMP and SAC-C provide the first measurements from space to accurately pinpoint the planetary boundary layer.

Without fly-wheeling, the receiver would lose the signal once the SNR drops below about 35, which, in the above example, would end the occultation after ~40 seconds and lose all information about the structure below 2 km. In fly-wheeling, when SNR < SNR_{cutoff} (=35-50), the receiver extrapolates the model for the signal Doppler and Doppler rate (to maintain its 3rd order phase-lock loop) based on data from the previous few seconds. The receiver will then record the real and imaginary correlation sums[4] based on which the SNR and phase difference between the received signal and the extrapolated model are computed. This continues until the SNR is > SNR_{cutoff} (after which the receiver goes back into close-loop mode) or 15 seconds have elapsed (after which the occultation is ended). During fly-wheeling, if the extrapolated Doppler used as a model remains sufficiently close to the average atmospheric Doppler to within ± half the receiver's sampling rate, (±25Hz for this example), then the recorded phase and amplitude would be the true phase and amplitude (plus noise) of the signal at the receiver. Signals with Doppler difference from the model, Δf, outside the ±25Hz bandwidth are still recoverable but are significantly weakened by the $\sin(\pi\Delta f T_s)/\pi\Delta f T_s$ filter, T_s is the sampling time (=1/50 seconds), introduced by the receiver.

[4] These are the real and imaginary sums of the product of the received signal sampled at 20 MHz and an internally generated model of the Coarse Acquisition (C/A) code of the GPS satellites [see Thomas, 1995]. The sums are over a 0.02 or 0.01 seconds corresponding to the sampling interval.

To further understand the dynamics of the signal and examine the degree of success of tracking it in the lower troposphere, occultation data was sampled at 100Hz from SAC-C during 5-Nov-2001 to 25-Jan-2002. (The normal rate is 50 Hz for CHAMP and SAC-C.) When sampled at 100Hz, the signal is recoverable if the fly-wheeling model remains within ±50Hz from the actual average atmospheric Doppler. Using a procedure suggested by Hajj et al., [2002b], it is possible to predict the atmospheric Doppler based on the separation angle between the occulted GPS and LEO satellites relative to the center of curvature of the geoid in the vicinity of the occultation tangent point (see Figure 13.a). This prediction is obtained independently of any atmospheric model and is now being implemented for open-loop tracking. However, for the time being, we use this predicted Doppler as a measure of how well the 'fly wheeling' is performing. Figure 13.b shows the difference of 1-sec average atmospheric Doppler and modeled Doppler (based on the bending of Fig. 13.a) as a function of the straight-line tangent point for 99 SAC-C occultations taken on 6-Nov-2001. Deviations of order ±10 Hz from the model reflect true structure in the atmosphere. Larger deviations can be attributed to the tracking loop; however, as long as the deviation does not exceed ± half the receiver's sampling rate (±50 Hz), the signal can be fully tracked.

Figure 13.a

Figure 13.b

When several tones are simultaneously observed, careful interpretation of the signal is needed to obtain accurate retrievals. As an example, these multiple tones can be seen in the power spectrum (Figure 14) of the occultation of figure 12. This spectrum is obtained by subtracting the atmospheric phase as recorded by the receiver from the modeled phase (as described above), and then taking the complex fast Fourier transform (FFT) with a 2 seconds moving window. The following features are seen in the spectrum: (1) One tone is dominant at the beginning of the occultation until 35 sec. (2) The signal splits into 2 or 3 tones between 35-38 sec., disappears between 38-46 sec. due to ducting and reappears with a broad spectrum (5-6 Hz) between 45-50 sec. (3) A tone appears at ~30 sec. and crosses the figure diagonally. This tone can be seen with various intensity in nearly all occultations. If was first observed in LEO to geostationary satellite occultations and interpreted as a surface reflection by Pavelyev et al., [1997]. Later observation from CHAMP and simulation of the reflected signal Doppler shift relative to the direct signal confirmed this interpretation [Beyerle and Hocke, 2001]. (4) A horizontal spread of power is observed at 25 sec., which is due to the receiver slipping several cycles at that time.

The various tones present in the spectrum are due to atmospheric multipath caused by the sharp refractivity gradient such as encountered around the tropopause and in the lower troposphere. To properly account and correct for atmospheric multipath, several approaches have been examined, including "backpropagation" and radio holography [Gorbunov, 2000], sliding spectrum [Sokolovskiy, 2001], and canonical transform [Gorbunov, 2001]. While these approaches can minimize the difficulties of dealing with multipath, they also impose limitations by reducing the signal to bending as a function of impact parameter, $\alpha(a)$. Strictly speaking, $\alpha(a)$ is singular at a point of total internal reflection (such as the top of the boundary layer). When performing the numerical Abel transform, interpolation across the $\alpha(a)$ singularity is required, which can result in under-

estimating the inverted refractivity. This negative N-bias was first observed by Rocken et al., [1997] and later evaluated by means of simulations by Sokolovskiy [2001]. The N-bias can be seen in the example of Figure 12.b where retrieved WVP stands lower than all radiosonde measurements and the NCEP analyses. It is also seen in Figure 7 where statistical comparisons of CHAMP and SAC-C refractivity to NCEP weather analyses are shown. The N-bias remains an open issue and further research is needed to fully understand its cause and to find ways to eliminate it.

7. CHAMP-SAC/C Cross Comparison

The presence of two missions concurrently collecting occultations provides the first opportunity to validate occultation data independent of a model and potentially assess the technique's claim to sub-K temperature accuracy. Even though, in the strictest sense, comparison of CHAMP and SAC-C will establish only a level of consistency between the two measurements, their often very different viewing geometries can cause them to be subject to quite different atmospheric propagation, asymmetry, and mismodeling effects, which can be a major source of error. Careful study of coincident soundings, particularly the closest in space and t`ime, can reveal a good deal about overall accuracy. Many sharp or unusual features observed in common by the two, from different viewpoints, can only be interpreted as real features in the atmosphere and are further indicative of accuracy.

In searching for coincident CHAMP and SAC-C occultations, we first consider all the data collected from these two satellites in the period August-22-2001 to October-15-2001 with a total of ~4200 CHAMP and ~6800 SAC-C occultations. In collocating CHAMP and SAC-C occultations, we must first decide on the proper time and space windows appropriate for two occultations to be considered "close". In determining these windows we first try to answer the following two questions: (a) how much does the atmosphere vary with time at a fixed location and (b) how much does it vary in space for a fixed time.

Atmospheric variation in time: We answer question (a) by the following procedure: (1) Find all CHAMP and SAC-C occultation pairs that are within 800 km distance and 3 hours from each other. (For the moment the distance is approximately determined based on the position of the tangent point at 30 km altitude.) The number of these pairs is ~1400. (2) For each pair, find the NCEP profile at the location of the CHAMP occultation at the two different times corresponding to the CHAMP and SAC-C occultations (a linear interpolation between the 12 hourly NCEP analyses is used)[5]. (3) We divide the occultation pairs in ½ hourly time bins and we form statistics for each bin. The mean and standard deviation of the temperature difference of all pairs within each bin are computed as a function of height and shown in Figure 15. This figure shows that changes of order 0.5 degrees are expected within 1.5 hrs. Because of the low time resolution of the model (12 hrs), we expect this estimate to be a lower bound of the real variability in the atmosphere; therefore, in answering question (b) above, we limit ourselves to occultations pairs that are in the first bin (i.e., < ½ hrs apart).

Figure 15

[5] Because the duration of an occultation is ~60 seconds, it is fair to assume that the atmosphere is not changing in any significant way during this time and to assign a single time to each occultation.

Atmospheric change with distance: In order to answer question (b) above, we consider the pairs of CHAMP-SAC/C occultations that are < ½ hrs apart (a total of ~300). Each pair is represented graphically by a line in Figure 16 showing the distance between the two occultations as a function of altitude (computed based on the estimated location of the tangent point for each occultation at that altitude). Next, for each pair, we obtain the corresponding NCEP profiles at the times and locations of the CHAMP and SAC/C occultations and compute the temperature difference between them as a function of altitude. Figure 17 is a scatter plot of the NCEP temperature differences obtained this way as a function of distance for all altitudes. Because of the very small change in temperature introduced by the model within ½ hr (leftmost panel of Figure 15), temperature changes in Figure 17 are mainly due to variation with distance. The root-mean-square (RMS) temperature difference in Figure 17 is less than 0.65 K for distances less than 200 km. As in the time variation estimate above, we expect this to represent a lower bound on the true gradient that can be observed in the atmosphere.

Figure 16

Figure 17

In summary, based on the NCEP analysis, temperature changes in the atmosphere within ½ hrs. and 200 km radius are less than ~0.65 K. Below we examine pairs of profiles within this time-space window in more detail.

Comparison of profiles within ½ hr. and 200 km window

For the period Aug. 22, 2001 to Oct. 15, 2001, there are only 15 profiles that are within ½ hr and 200 km apart as seen in Figure 16. Of these 15, we examine 8 in detail selected at different latitudes with noteworthy features. Panels a-h of Fig. 18 correspond to the lines marked a-h in Figure 16. Each example in Figure 18 also shows the NCEP and ECMWF analyses interpolated to the locations and times of CHAMP and SAC-C, the average latitude and longitude of the occultation pair, the average orientation, and the IDs of the occultations involved. Starting with the high northern latitude region, Figure 18.a shows close agreement between the CHAMP and SAC-C profiles at nearly all heights, but especially near the tropopause. On the other hand, the temperature structure around the tropopause is conspicuously different for the NCEP and ECMWF analyses, which tend to smooth sharp structures and thus overestimate the temperature at the tropopause. In this example, because the differences between CHAMP and SAC-C are < 0.5 K everywhere below 20 km altitude, while it is significantly larger (1-3 K) between the occultation profiles and the analyses around and above the tropopause, the discrepancy is very likely due to smoothing biases in the analyses. The close agreement between CHAMP and SAC-C – different instruments with different antennas and viewing geometries – tends to support expectations based on early theoretical studies [Kursinski et al., 1997].

Figure 18

Similar features are seen in the examples of 18.b and 18.c taken at high northern latitudes. As in the example of 18.a, the analyses are smoothing the structure around the tropopause resulting in an overestimate (underestimate) below (above) the tropopause. We note that in 18.b the difference between the CHAMP and SAC-C temperatures at the tropopause is nearly equal to the temperature difference between the corresponding NCEP profiles at the same altitude, suggesting that the gradient could very well be real. A similar but larger gradient is seen in the occultation pair than in the analyses in the

example of 18.c. We further note that there is a significant correlation between the CHAMP and SAC-C wavy structures in the stratosphere in both examples of 18.b and 18.c suggesting that these waves are real. By contrast, these waves are significantly reduced or absent in the analyses. In all examples of 18.a-c, the lapse rates above and below the tropopause are significantly larger in the occultation profiles than in the analyses.

Moving to high southern latitude, we show the three examples in 18.d-f. Some of the common features are: (1) CHAMP and SAC-C are significantly closer to each other than they are to the analyses. (2) Temperature lapse rates agree very well between CHAMP and SAC-C in the troposphere but deviate significantly from the analyses (Figs. 18.d and 18.e below 10 km). (3) Sudden changes in the temperature lapse rate reflecting the higher vertical resolution which is missed by the analyses. These changes match almost exactly between CHAMP and SAC-C (e.g., structures at ~2 km and 5 km in 18.d and at ~7 km in 18.e). (4) The CHAMP and SAC-C temperatures near the surface in 18.e (the Antarctic surface is at ~4 km altitude) and 18.f[6] are significantly higher (lower) than indicated by the NCEP (ECMWF) analyses. While we cannot draw a conclusion on a possible systematic bias in the analyses of the surface temperature in Antarctica from only two examples, identifying such a bias could be of importance in the detection of warming trends in that region. (5) In the stratosphere, there is a clear correlation in the wavy structure captured by CHAMP and SAC-C and a significant deviation from the analysis.

We finally consider two examples at low- (18.g) and mid-latitudes (18.h). In 18.g we see a significant temperature gradient between the CHAMP and SAC-C occultation near the tropopause which is absent in the analyses. If this gradient is real, it would be hard to capture with the analysis since the two occultations are only ~120 km apart (Figure 16), or within one grid in the analyses. Given the level of accuracy of GPS occultation near the tropopause, as suggested by previous examples, the observed gradient is likely to indicate a real temperature gradient in the atmosphere.

Statistical Comparison

To quantify the difference between CHAMP and SAC-C temperature measurements in a statistical sense, we expand our search for coincident occultations to the entire period common to CHAMP and SAC-C to date (covering July 10, 2001 to June 9, 2002). We limit our search to occultations that satisfy both criteria: (1) they occur less than ½ hour apart, (2) the tangent points of the two occultations are less than 200 km at least for one height. (The latter condition implies that some points are more than 200 km apart.) The data searched contains ~37000 CHAMP and ~38000 SAC-C occultations that were successfully retrieved. The number of pairs found that satisfy the two criteria mentioned above are 60. Combining these 60 pairs of coincident occultations into a set *S*, each point in *S* is characterized by the following:

[6] The somewhat jagged CHAMP and SAC-C temperature structure is most likely due to the dry-wet ambiguity present when the temperature is higher than 250K.

i index of the CHAMP-SAC/C pair (1 to 60)

h a tangent point height

$\vec{x}_{1,i}(h), \vec{x}_{2,i}(h)$ positions of a tangent point at height h for CHAMP and SAC-C, respectively, for pair i

$d_i(h)$ distance ($\left|\vec{x}_{1,i} - \vec{x}_{2,i}\right|$) between tangent points

$t_{1,i}$, $t_{2,i}$ times of the CHAMP and SAC-C occultations, respectively, for pair i

$T_{champ,i}(h)$ CHAMP retrieved temperature at height h, location $\vec{x}_{1,i}$ and time t_1 for pair i

$T_{sac\text{-}c,i}(h)$ SAC-C retrieved temperature at height h, location $\vec{x}_{2,i}$ and time t_2 for pair i

$T_{ncep@champ,i}(h)$ NCEP temperature at h, $\vec{x}_{1,i}$ and $t_{1,i}$

$T_{ncep@sac\text{-}c,i}(h)$ NCEP temperature at height h, $\vec{x}_{2,i}$ and $t_{2,i}$

In order to quantify temperature variation with distance, in Figure 19 we plot (ΔT_{gps} = $T_{champ,i}$- $T_{sac\text{-}c,i}$) as a function of d for all points in S with h between 0 and 18 km, a region where T is expected to be most accurate. A clear growth of ΔT_{gps} is seen with distance. Also indicated on the figure is the RMS of ΔT_{gps} vs. d. In the limit where the distance is < 50 km, the RMS is = 0.83 K. Since this would results from the sum of two independent errors, and assuming that CHAMP and SAC-C random errors are comparable, then the RMS error on each measurement is = $0.83/\sqrt{2}$ = 0.59 K. This number includes the occultation temperature errors and atmospheric variability in space (within 50 km radius) and time (within ½ hrs). To estimate the latter, we compute the RMS difference between ($T_{ncep@champ,i}$- $T_{ncep@sac\text{-}c,i}$) for the same set of points considered above and find it = 0.16K. This reduces the RMS error of GPS derived temperature to 0.57K.

Figure 19

As an alternative way for inferring the accuracy of temperature from CHAMP and SAC-C, we examine a histogram of ΔT_{gps} for all points in S satisfying d < 150 km and h between 5-10 km (Figure 20). To obtain robust statistics less sensitive to outliers (due, for example, to sharp temporal or spatial temperature variation), we use the median and the 68% confidence interval as measures of the mean and standard deviation in ΔT_{gps}. The 68% confidence interval is defined as the range centered around the median that contains 68% of the counts in Figure 20. (In a Guassian distribution the 68% confidence interval equals the standard deviation.) In the example of Figure 20, the median (m) and the 68% confidence interval (σ) are 0.04 and 0.82 K, respectively. These statistics reflect (1) measurement errors, and (2) spatial and temporal variation due to sampling the atmosphere at slightly different locations and times. In order to separate the two effects, we express the measured CHAMP and SAC-C temperatures as follows:

Figure 20

$$T_{champ}(\vec{x_1}, t_1) = T(\vec{x_1}, t_1) + \varepsilon_{champ} \quad (1.a)$$

$$T_{sac-c}(\vec{x_2}, t_2) = T(\vec{x_2}, t_2) + \varepsilon_{sac-c} \quad (1.b)$$

where $T(\vec{x}, t)$ represents the true temperature at $\vec{x}$, t; ε_{champ}, and $\varepsilon_{sac\text{-}c}$ are the CHAMP and SAC-C temperature errors including biases. Based on Eq. (1), the mean and standard deviation of the CHAMP and SAC-C temperature difference can be written as

$$m_{\Delta T_{gps}} = m_{atm} + \bar{\varepsilon}_{champ} - \bar{\varepsilon}_{sac-c} \tag{2.a}$$

$$\sigma^2_{\Delta T_{gps}} = \sigma^2_{atm} + \sigma^2_{champ} + \sigma^2_{sac-c} = \sigma^2_{atm} + 2\sigma^2_{leo} \tag{2.b}$$

where

$$m_{atm} = \text{mean}\left[T(\vec{x_1}, t_1) - T(\vec{x_2}, t_2)\right];\ \ \sigma^2_{atm} = \text{var}\left[T(\vec{x_1}, t_1) - T(\vec{x_2}, t_2)\right] \tag{2.c}$$

In the second equation of 2.b we have assumed that the measurement errors from CHAMP and SAC-C have the same variance.

To get a handle on the degree of atmospheric variability in space and time as reflected in m_{atm} and σ_{atm}, we turn to the NCEP analysis. We define

$$m_{ncep} = \text{mean}\left[T_{ncep}(\vec{x_1}, t_1) - T_{ncep}(\vec{x_2}, t_2)\right];\ \ \sigma^2_{ncep} = \text{var}\left[T_{ncep}(\vec{x_1}, t_1) - T_{ncep}(\vec{x_2}, t_2)\right] \tag{3}$$

and conjecture that

$$\sigma^2_{atm} > \sigma^2_{ncep} \tag{4}$$

$$m_{atm} \approx m_{ncep} \tag{5}$$

Eq. (4) implies that the model underestimates the true variability of the atmosphere. Eq. (5) implies that, even if the analysis is biased, there is little ground to believe that temperature difference between nearby grids are biased. Using Eqs. (2), (4) and (5), we can write

$$\sigma^2_{leo} = \frac{1}{2}(\sigma^2_{\Delta T_{gps}} - \sigma^2_{atm}) < \frac{1}{2}(\sigma^2_{\Delta T_{gps}} - \sigma^2_{ncep}) \tag{6.a}$$

$$\bar{\varepsilon}_{champ} - \bar{\varepsilon}_{sac-c} = m_{\Delta T_{gps}} - m_{atm} \approx m_{\Delta T_{gps}} - m_{ncep} \tag{6.b}$$

Since σ^2_{atm} is not directly available to us but σ^2_{ncep} can be computed from the analysis, Eq. (6.a) sets an upper bound on the error of GPS-LEO occultation measurements by CHAMP and SAC-C.

Figure 21 shows the right-hand side (RHS) of the inequality of (6.a) as a function of height and cutoff distance $\bar{d}$ ($\bar{d}$ =100 to 300 km in steps of 50 km). In computing the RHS of Eq. (6.a) for a given height $\bar{h}$ and distance cutoff $\bar{d}$, all points in *S* satisfying $\left|h - \bar{h}\right| < 5km$ and $d < \bar{d}$ are chosen and the median and 68% confidence interval are computed. As $\bar{d}$ approaches 0, the standard deviation curve becomes smaller and approaches the uncertainty in the GPS occultation temperature measurements. This is expected based on Eq. (6.a) since σ^2_{ncep} would reach 0. The 68% confidence interval curve associated with 100 km, therefore, represents an upper bound on the standard deviation of GPS occultation error and shows a σ_{leo} <0.5K between 5-18 km. The error grows to ~1K between 18 and 30 km altitudes. The curve does not extend to the surface because we exclude regions in the troposphere where T > 250 K to avoid the dry/moist term ambiguity.

Figure 21

Similarly, we can infer the mean difference between CHAMP and SAC-C by computing the RHS of Eq. (6.b). The results are shown in Fig. 21 for similar cutoff distances as

before. Mean differences are less than 0.1 K at all heights between 5-30km, reflecting the precision of averaged GPS profiles. Even smaller differences may be seen when averaging over larger data sets (60 or less were used here) used for climate variability studies. This result tends to support one of the more dramatic claims made for GPS sounding in early analytical studies [Kursinski et al., 1997]– that its inherently low bias and high precision can provide regional temperature averages accurate to better than 0.1 K (or 1 part in 3000), enabling for the first time the detection of ongoing climatic change over a period of a few years, with a technique that is at once efficient, global, and all-weather.

Estimated Errors in the Analysis

Having obtained a σ on temperature errors from GPS occultations, it is now possible to infer the σ of the analysis temperature errors. We do this by computing the mean, median, standard deviation and 68% confidence interval of the temperature differences between CHAMP or SAC-C and the corresponding NCEP temperature interpolated to the location and time of the occultation. The left panel of Fig. 22 plots these statistics for both CHAMP and SAC-C, showing differences of order 0.1-0.25K in the mean(median) and 1-2.5K in standard deviation(68% confidence interval). Using the 68% confidence interval statistics for CHAMP and SAC-C from this figure and the estimated GPS occultation temperature error (curve corresponding to 100km in Figure 21), we estimate the overall error of the NCEP analysis to be of order 1-1.6 K (right panel of Figure 22), though this can reach considerably greater values near sharp features, such as the tropopause.

Figure 22

8. Summary and Conclusion

To date, over 10^5 CHAMP and SAC-C occultations have been collected and processed to yield high quality temperature profiles in the troposphere and the stratosphere. These occultations are obtained during a time when the GPS L2 signal is encrypted. Comparisons to weather analysis indicates that the quality of retrievals is not degraded compared to data collected from the GPS/MET experiment during periods when the encryption of the GPS signal was temporarily disabled. This is made possible by a new generation of GPS flight receivers employing advanced "semi-codeless" techniques and is vital to establish GPS sounding as a powerful new tool for climate and weather research.

The two missions produce on average 350 daily global occultations. This number will approach the expected level of 500 as various failure modes are evaluated and fixed. Future software uploads and the enabling of GPS occultations on GRACE will bring the number of daily soundings to over 1200, surpassing the total of semi-daily radiosonde profiles.

The enhanced tracking loop in the lower troposphere currently enables the signal to reach to the lower 0.5 km for ~60% of the time globally (35% in the tropics and 85% at latitudes > 60 deg.). This is a considerable improvement of the performance of

GPS/MET and this number is expected to reach 90-95% when the "open loop" tracking is implemented. As demonstrated, GPS occultation offer the first remote sensing measurements to sense the PBL top with a very high vertical resolution.

Collection of precise GPS soundings concurrently from two platforms has enabled for the first time direct inter-comparisons of profiles. Our analysis shows that temperature profiles collected from CHAMP and SAC-C are consistent to 0.05-0.1K in the mean and 0.5K in standard deviation. This precision surpasses that of all other spaceborne instruments and is naturally free of long term drifts, making GPS sounding ideally suited to detecting weak climate signals in a relatively short time. Assuming a 0.2 K/decade temperature increase – the mid-point of IPCC estimates for human-driven warming [Houghton et al., 1990, p. 248] – and a GPS measurement precision and stability of < 0.1 K for climatic temperature averages, we can expect to detect the climate signal within about 5 years.

Given the many planned missions to collect GPS soundings in the next decade, including COSMIC, ACE+, EQUARS, NPOESS, and other flights of opportunities, the density of coverage will become sufficient for a wide range of climate and weather applications, including establishing detailed baseline climatologies; conducting studies of diverse climate process, such as stratosphere-troposphere exchange and tropical convection; testing climate models; and detecting climatic change. It is envisaged that GPS soundings will soon become a vital input both to general circulation models and to numerical weather models and will trigger improvements in a range of environmental predictions, from tomorrow's weather forecast to seasonal climate variations to long-term climatic change.

Acknowledgement

This work was performed at the Jet Propulsion Laboratory, California Institute of Technology, under a contract with the National Aeronautic and Space Administration.

References

Bertiger, W. I., Y. E. Bar-Sever, E. J. Christensen, E. S. Davis, J. R. Guinn, B. J. Haines, R. W. Ibanez-Meier, J. R. Jee, S. M. Lichten, W. G. Melbourne, R. J. Muellerschoen, T. N. Munson, Y. Vigue, S. C. Wu, and T. P. Yunck, B. E. Schutz, P. A. M. Abusali, H. J. Rim, M. M. Watkins, and P. Willis, "GPS Precise Tracking Of Topex/Poseidon: Results and Implications," *JGR Oceans Topex/Poseidon Special Issue*, vol. 99, no. C12, pg. 24,449-24,464 Dec. 15, 1994.

Beyerle, G., and K. Hocke, Observation and simulation of direct and reflected GPS signals in radio occultation experiments, Geophys. Res. Lett., 28 (9): 1895-1898 MAY 1 2001.

De la Torre Juarez, M., G. A. Hajj, E. R. Kursinski, D. Kuang, A. J. Mannucci and L. J. Romans, Single frequency processing of atmospheric radio-occultations, submitted to *International Journal of Remote Sensing,* 2002.

Fjeldbo, G. F., V. R. Eshleman, and A. J. Kliore, The neutral atmosphere of Venus as

studied with the Mariner V radio occultation experiments, Astron. J., 76, 123-140, 1971.

Gorbunov M. E., A. S. Gurvich, L. Kornblueh, Comparative analysis of radioholographic methods of processing radio occultation data, Radio Sc., 35(4), 1025-1034, 2000.

Gorbunov, M.E., Gurvich, A.S., Bengtsson, L., Advanced algorithms of inversion of GPS/MET Satellite data and their application to reconstruction of temperature and humidity. Max-Planck-Institute fur Meteorologie Report No. 211. F.R. Germany, August, 1996.

Gorbunov M. E., Radioholographic methods for processing radio occultation data in multipath regions, Danish Meteorological Institute Scinentific Report, 01-02, Copenhagen, 2001.

Hajj, G. A., E. R. Kursinski, W. I. Bertiger, L. J. Romans, and K. R. Hardy, Assessment of GPS occultations for atmospheric profiling, in *Proc. Of the 7th conf. on satellite meteorology and oceanography,* Monterey, CA., American Meteorlogical Society, June 6-10, 1994.

Hajj, G. A., M. de la Torre Juarez, B. A. Iijima, E. R. Kursinski, A. J. Mannucci, and T. P. Yunck, GPS radio occultations coming of age: spacecraft launches add two new instruments for climate monitoring, EOS, Transactions, Vol. 83, No. 4, p. 37, 22 Jan. 2002a.

Hajj, G. A., E. R. Kursinski, L. J. Romans, W. I. Bertiger, S. S. Leroy, A technical description of atmospheric sounding by GPS occultation, *J. of Atmos. And Sol.-Terr. Phys.,* 64, pp 451-469, 2002b

Hajj, G. A., E. R. Kursinski, W. I. Bertiger, S. S. Leroy, T. Meehan, L. J. Romans, and J. T. Schofield, Initial results of GPS-LEO occultation measurements of Earth's atmosphere obtained with the GPS/MET experiment, Proc. IAG Symp. G1, GPS Trends in Precise Terrestrial, Airborne, and Spaceborne Applications, IUGG XXI General Assy., Boulder, CO, 2-14 July 1995, Springer-Verlag, 1996.

Houghton, J. T., G. J. Jenkins and J. J. Ephraums (eds.), *Climate Change, The IPCC Scientific Assessment*, Univ. of Cambridge, Cambridge, England, 1990.

Karayel E. T., D. P. Hinson, Sub-Fresnel-scale vertical resolution in atmospheric profiles from radio occultation, Radio Sci., 32(2), 411-423, 1997.

Kuang, D., Y. Bar-Sever, W. I. Bertiger, S. S. Desai, B. J. Haines, B. A. Iijima, G. L. Kruizinga, T. Meehan, L. J. Romans, Precise Orbit Determination for CHAMP using GPS Data from BlackJack Receiver, Proceedings of ION National Technical Meeting 2001, Long Beach, California, January 24, 2001.

Kursinski, E. R, G. A. Hajj, W. I. Bertiger, S. S. Leroy, T. K. Meehan, L. J. Romans, J. T. Schofield, D. j. McCleese, W. G. Melbourne, C. L. Thornton, T. P. Yunck, J. R. Eyre, and R. N. Nagatani, Initial results of radio occultation observations of Earth's atmosphere using the Global Positioning System, Science, 271, 1107-1110, 1996.

Kursinski, E. R., G. A. Hajj, K. R. Hardy, J. T. Schofield, and R. Linfield, Observing Earth's atmosphere with radio occultation measurements, J. of Geophys. Res., 102(D19), 23429-23465, 1997.

Kursinski, E. R., G. A. Hajj, K. R. Hardy, L. J. Romans and J. T. Schofield, Observing tropospheric water vapor by radio occultation using the Global Positioning System, Geophys. Res. Lett., 22, 2365-2368, 1995.

Kursinski, E. R. and G. A. Hajj, A comparison of water vapor derived from GPS occultations and global weather analyses, *J. Geophys. Res.,* 106(D1), pp. 1113-1138,

2001.
Leroy, S. S., Measurement of geopotential heights by GPS radio occultation, J. Geophys. Res., 102, 6971-6986, 1997.
Melbourne, W. G., E. S. Davis, C. B. Duncan, G. A. Hajj, K. R. Hardy, E. R. Kursinski, T. K. Meehan, L. E. Young, and T. P. Yunck, The application of spaceborne GPS to atmospheric limb sounding and global change monitoring, JPL Publ. 94-18, Pasadena, California, April 1994.
Pavelyev A., A.I. Zakharov, A.I. Kucherjavenkov, E.P. Molotov, A.I. Sidorenko, I.L. Kucherjavenkova and D.A. Pavelyev, Propagation of Radio Waves Reflected from Earth's Surface at Grazing Angles between a Low-Orbit Space Station and a Geostationary Satellite. *Journal of Communication Technology and Electronics.* **42,** No. 1. P. 51-57**.** 1997.
Rocken, C., R. Anthes, M. Exner, D. Hunt, S. Sokolovskiy, R. Ware, M. Gorbunov, W. Schriener, D. Feng, B. Herman, Y.-H. Kuo, X. Zou, Analysis and validation of GPS/MET data in the neutral atmosphere, J. Geophys. Res., 102(D25), 29,849-29,866, 1997.
Sokolovskiy, S.V., Inversions of radio occultation amplitude data. Radio Science 35(1), pp. 97-105, 2000.
Sokolovskiy, S. V., Modeling and inverting radio occultation signals in the moist troposphere, Radio Sci., 36(3), 441-458, 2001.
Thomas, J. B., Singal-Processing Theory for the TurboRogue Receiver, JPL Publication 95-6, April, 1995.
Ware, R., Exner M. Feng D. Gorbunov M. Hardy K. Herman B. Kuo Y. Meehan T. Melbourne W., Rocken C., Schreiner W., Sokolovskiy S., Solheim F., Zou X., Anthes R., Businger S., Trenberth K., GPS sounding of the atmosphere from low earth orbit: Preliminary results, Bull. Am. Meteorol. Soc., 77(1), 19-40, 1996.
Wickert J., G. Beyerle, G. A. Hajj, V. Schwieger, C. Reigber, GPS radio occultation with CHAMP: Atmospheric profiling utilizing the space-based single difference technique, *Geophys. Res. Lett.,* to appear, 2002
Wickert, J., Reigber C., Beyerle G., Konig R., Marquardt C., Schmidt T., Grunwaldt L., Galas R., Meehan T. K., Melbourne W. G., Hocke K., Atmosphere sounding by GPS radio occultation: First results from CHAMP, *Geophys. Res. Lett*., 28(17) 3263-3266, 2001.
Wu, S. C., T. P. Yunck, and C. L. Thornton, Reduced-dynamic technique for precise orbit determination of low Earth, *J. Guid. Control Dyn., 14*(1), 24–30, 1991.
Yunck, T. P., G. F. Lindal, and C. H. Liu, The role of GPS in precise earth observation, paper presented at the IEEE Position, Location and Navigation Symposium, Orlando, Fl., Nov. 29-Dec. 2, 1988.
Yunck, T. P., S. C. Wu, J. T. Wu, C. L. Thornton, Precise tracking of remote sensing satellites with the Global Positioning System, *IEEE Trans Geosci Rem Sens* (28), Jan 1990.

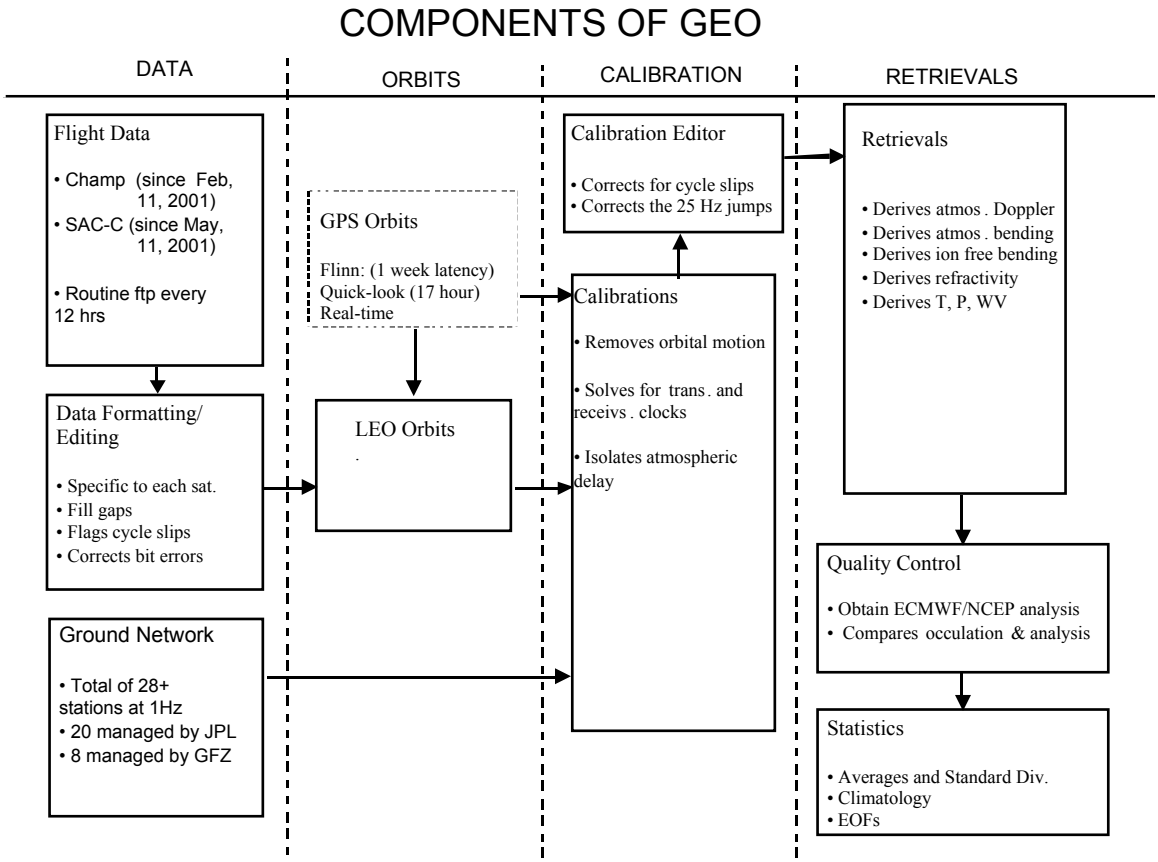

Figure 1: An overview of the GPS Earth Observatory (GEO) system at JPL used for routine processing of GPS occultation data.

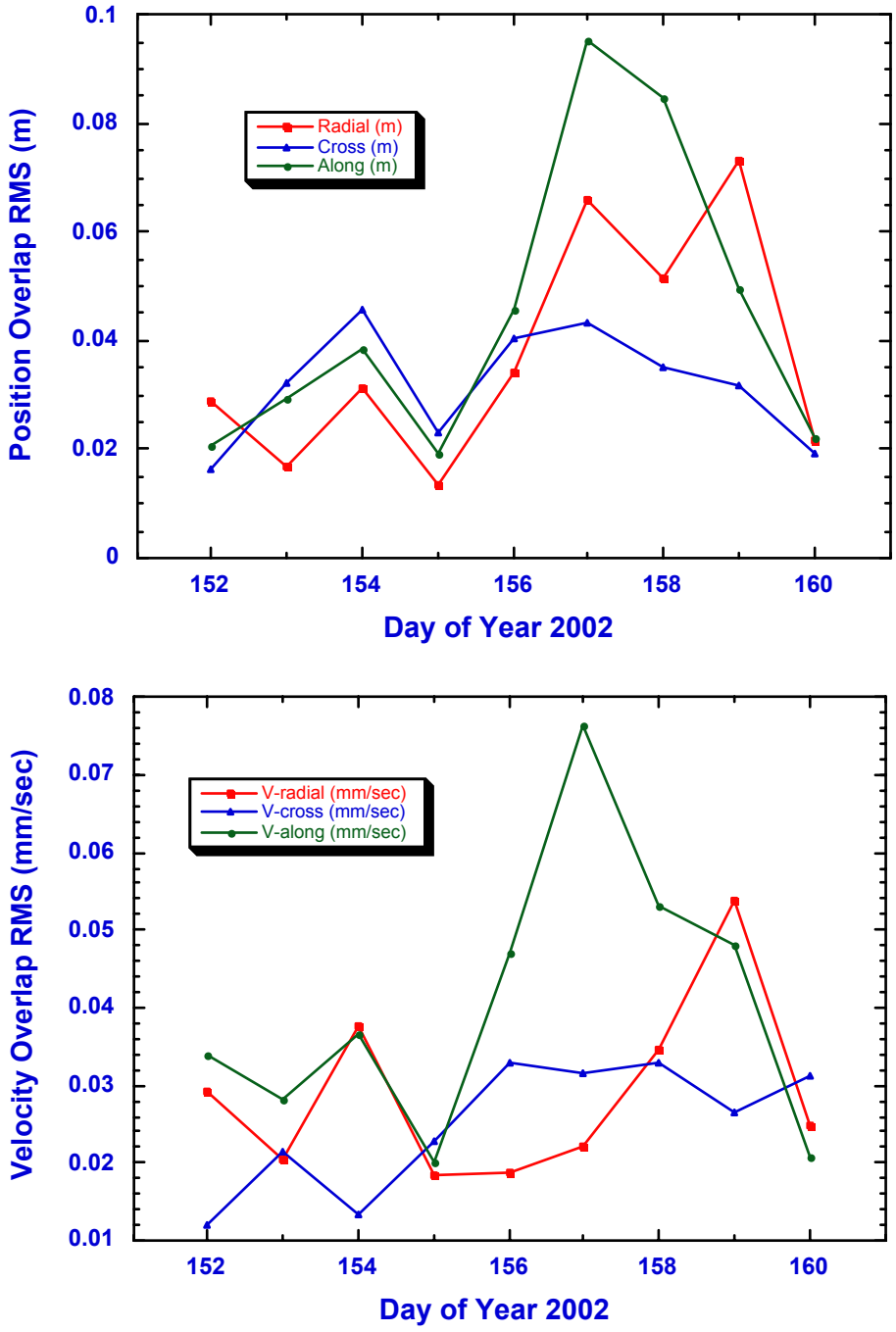

Figure 2. Daily RMS of radial, cross-track and along-track orbital overlap differences for CHAMP position (top) and velocity (bottom).

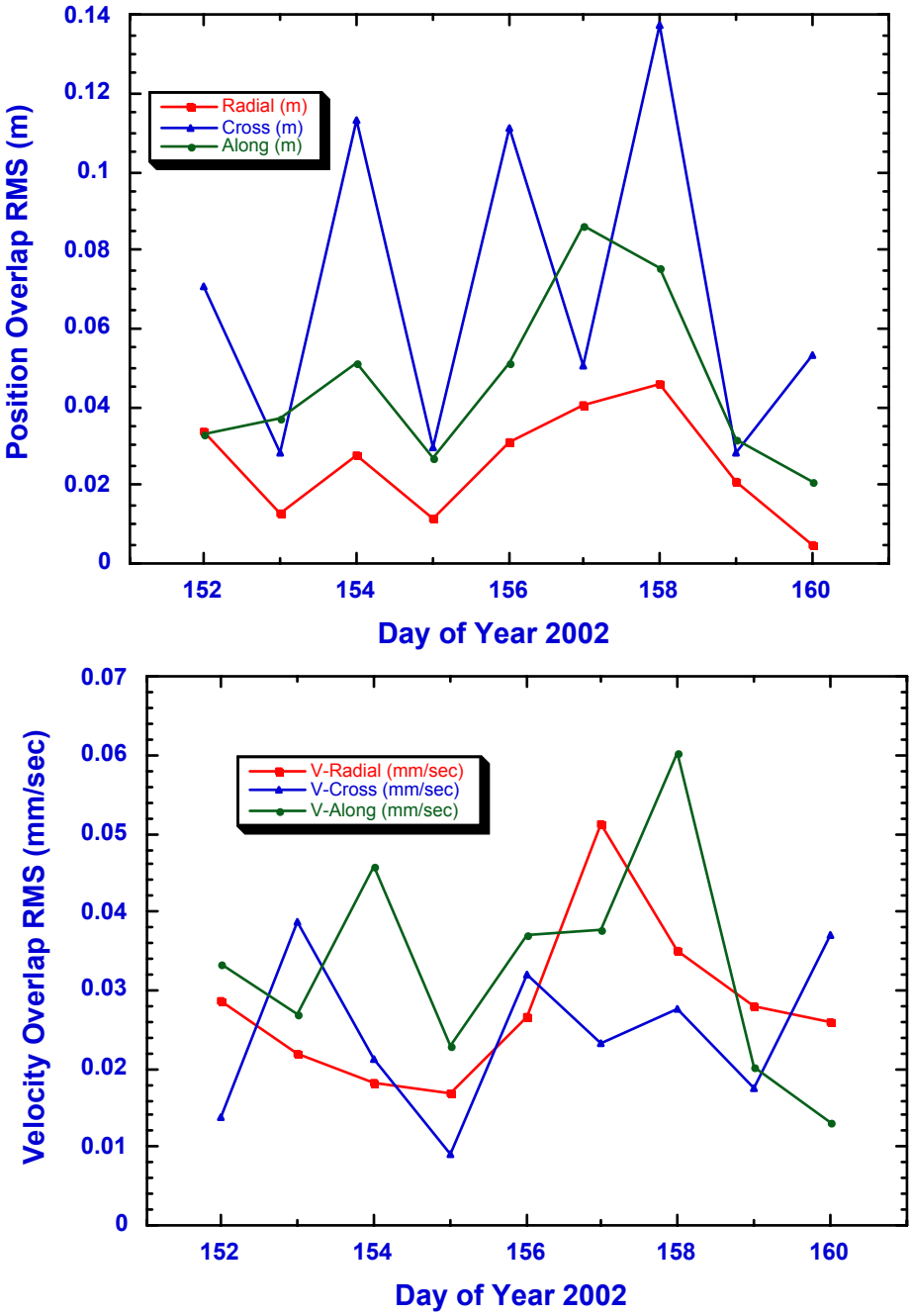

Figure 3. Same as Figure 2 but for SAC-C.

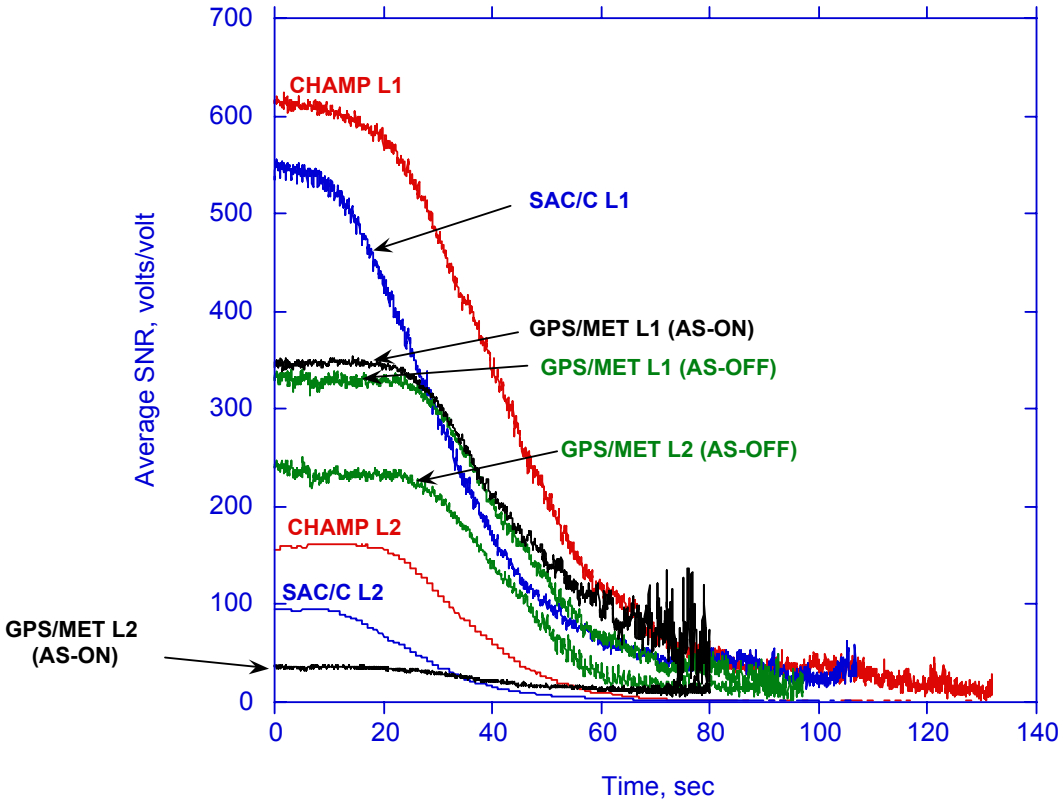

Figure 4: Average voltage signal-to-noise ratio (SNR) for the occulted link at the two GPS frequencies (L1 and L2) for various satellites and under various conditions (AS on and off). Each curve is an average over nearly 200 occultations collected in a day.

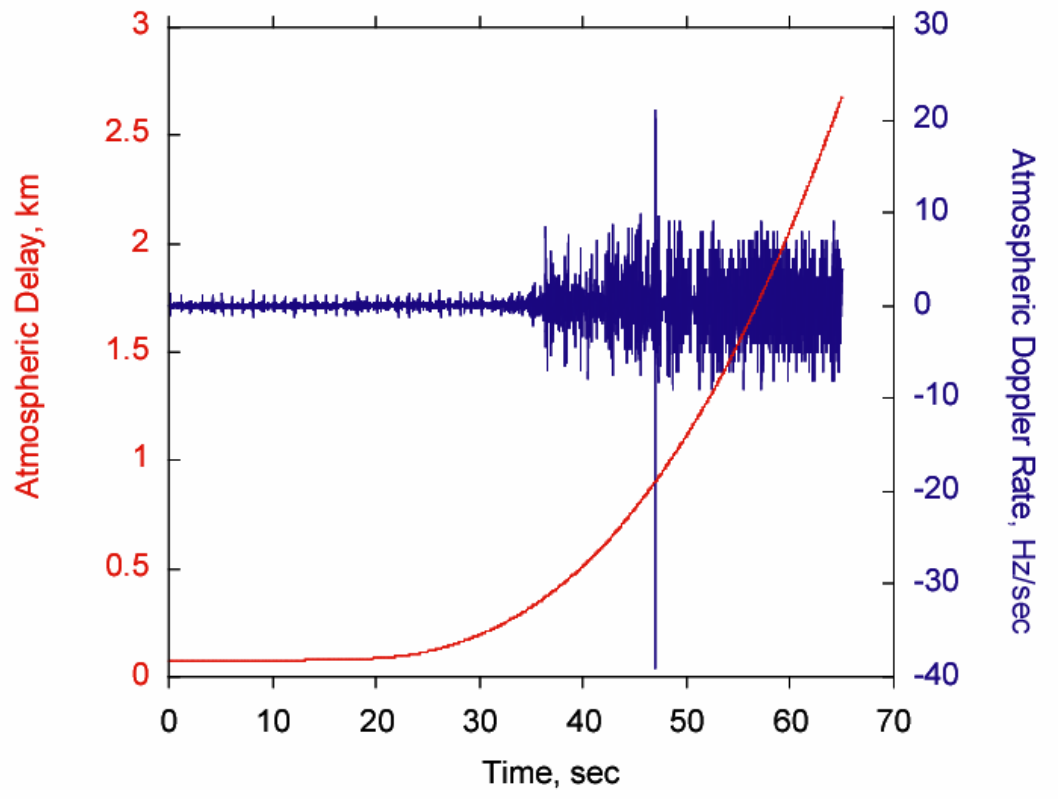

Figure 5: Phase delay (left scale) and acceleration (right scale) for a CHAMP occultation.

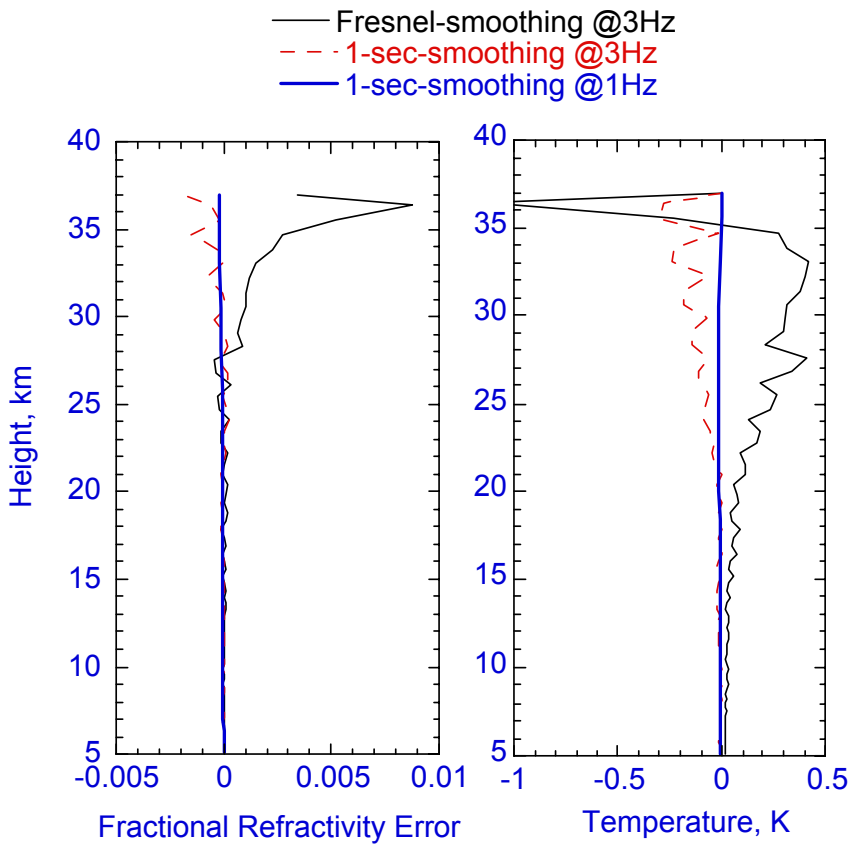

Figure 6: Fractional refractivity and temperature difference between two profiles derived from "noisy" and "smooth" phase measurements for three different smoothing windows and sampling rates.

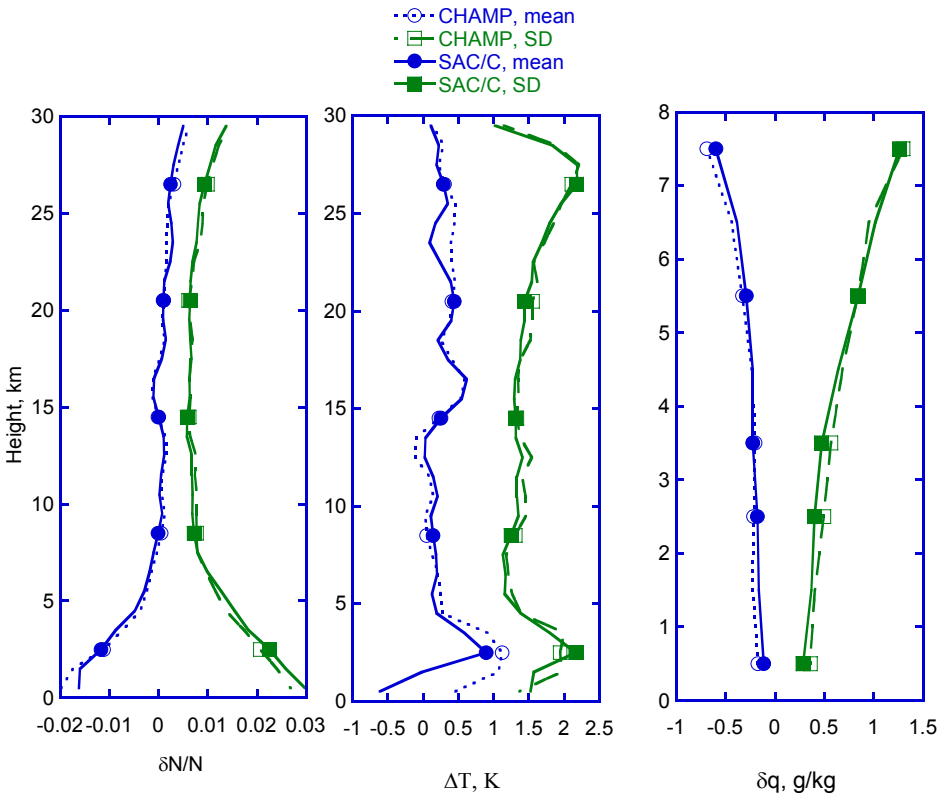

Figure 7: Means of standard deviations of fractional refractivity (left), temperature (middle) and specific humidity (right) differences between SAC/C (solid curves) or CHAMP (dashed curves) and NCEP analysis interpolated to the locations and times of the occultations. Statistics is based on occultations collected during the period June 1-7, 2002. The coverage for this period is shown in Figure 9.

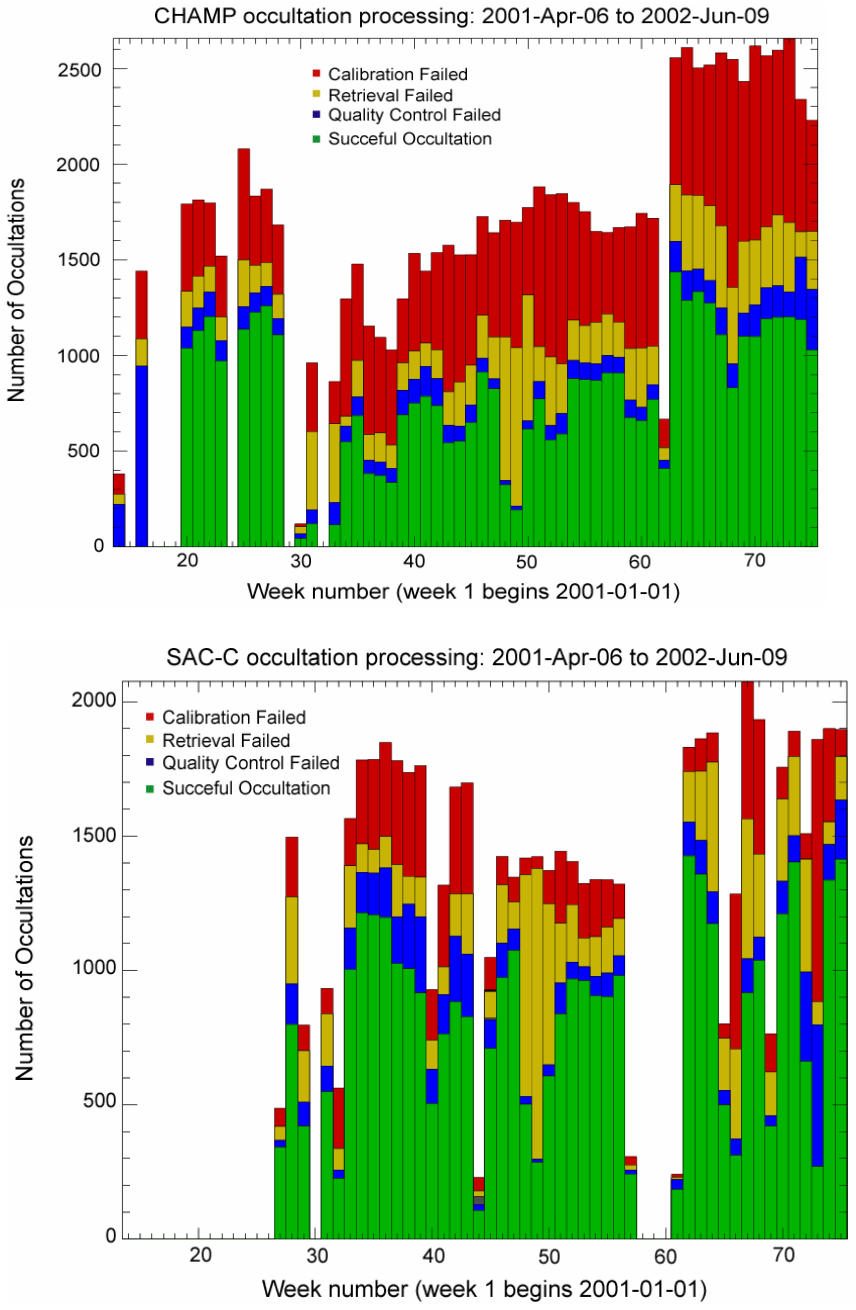

Figure 8: Total weekly number of occultation since the beginning of the CHAMP and SAC-C missions. The different colors indicate different failure modes in the processing of the occultations. The top of the red bars indicate the total number of occultation scheduled by the receiver. The top of the green bar indicate the number of those that passed all stages of the processing system including quality control. Gaps correspond to days where the receiver was not turn on.

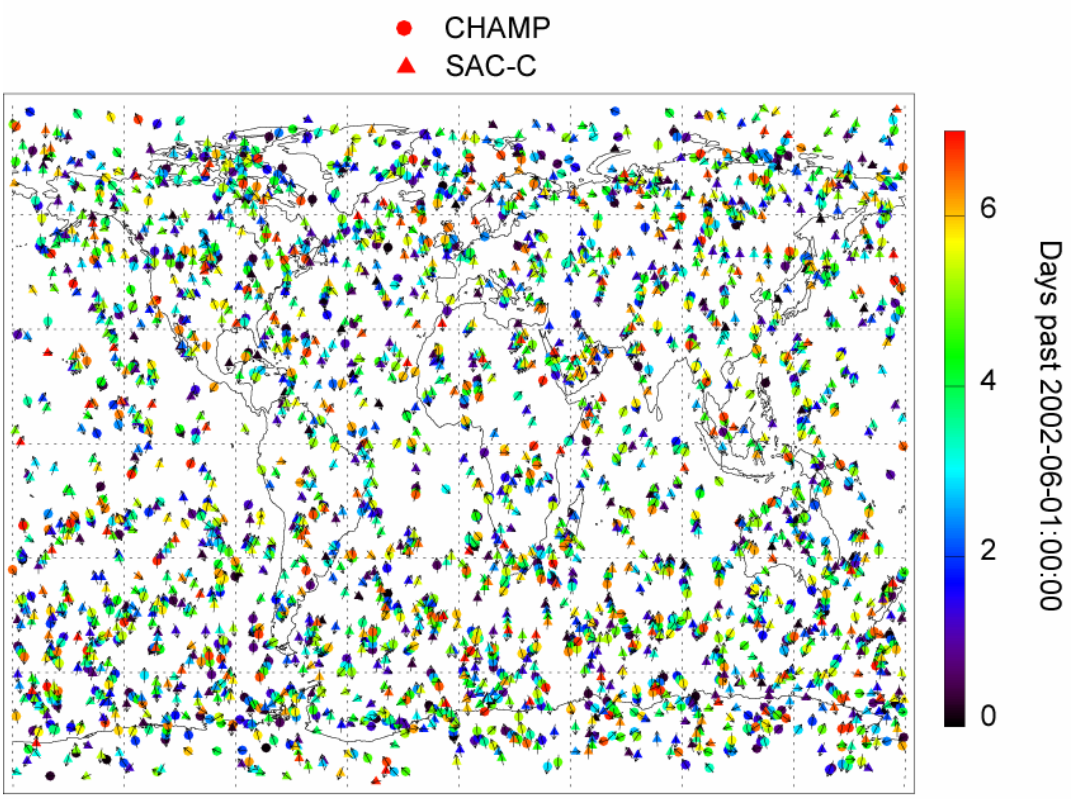

Figure 9: Map of CHAMP (circles) and SAC-C (triangles) occultation coverage for one week starting at mid-night of June 1, 2002. Only occultations that passed the quality control (a total of ~2500 for both satellites) are shown. The color indicates the time according to the color bar spanning the period from 0-7 days. The arrow indicates the occultation orientation.

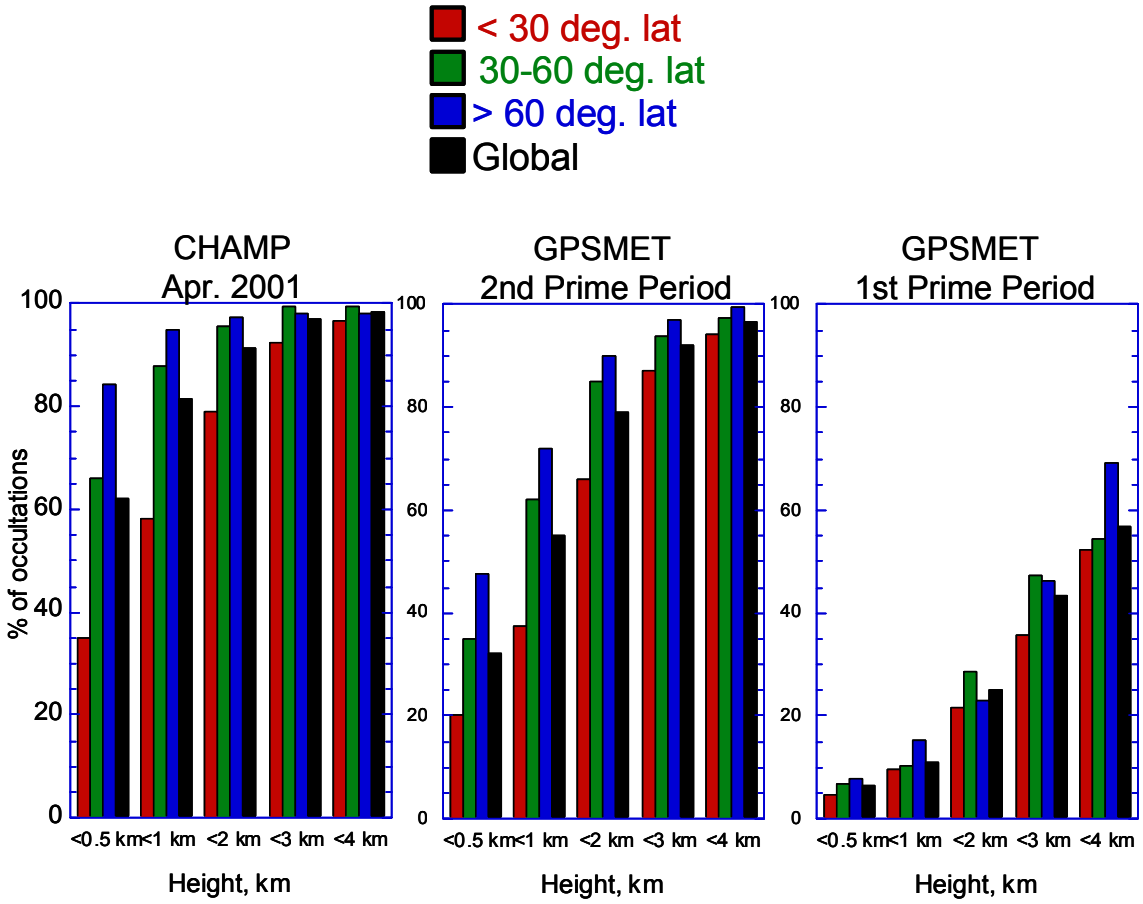

Figure 10: Percentages of occultations penetrating below a specified height for different latitude bands and globally. This shown for CHAMP based on 900 early CHAMP occultations (left), and compared to the second (middle) and first (right) prime periods from GPS/MET.

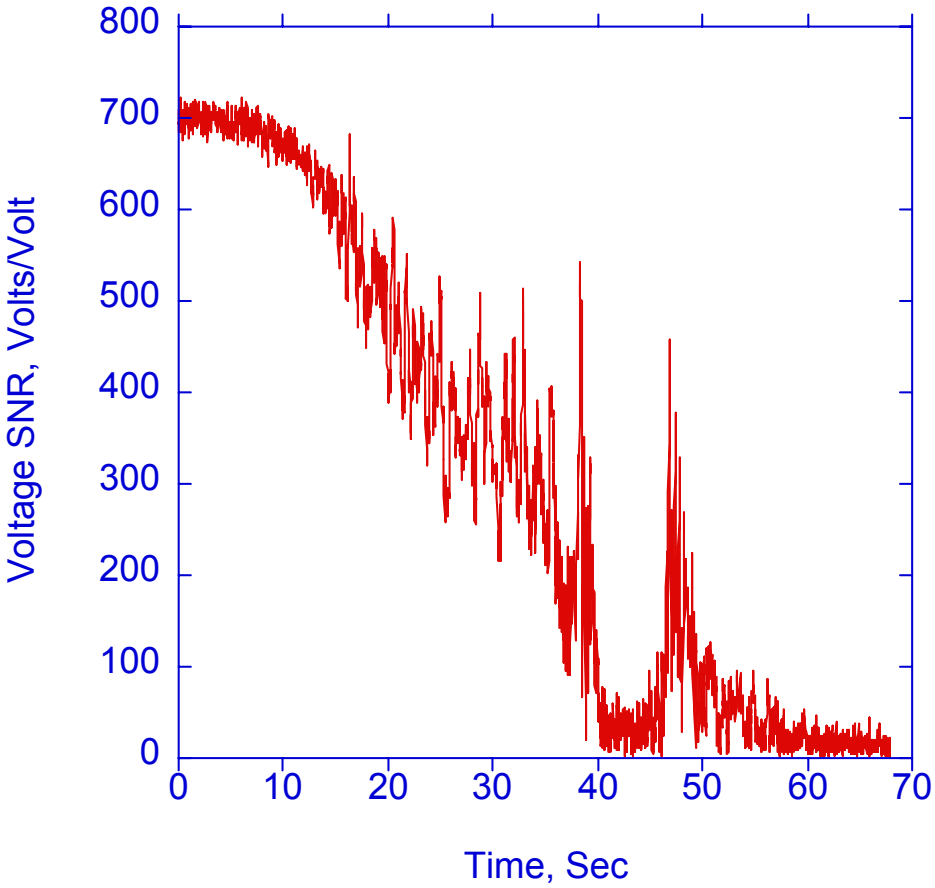

Figure 11: Signal-to-noise ratio of a CHAMP occultation as a function of time showing the disappearance of the signal for a during of ~8 seconds commencing at the time when the occulted signals' tangent height is immediately below the top of the planetary boundary layer. The signal reemerges when the conditions for total internal reflaction are no longer satisfied.

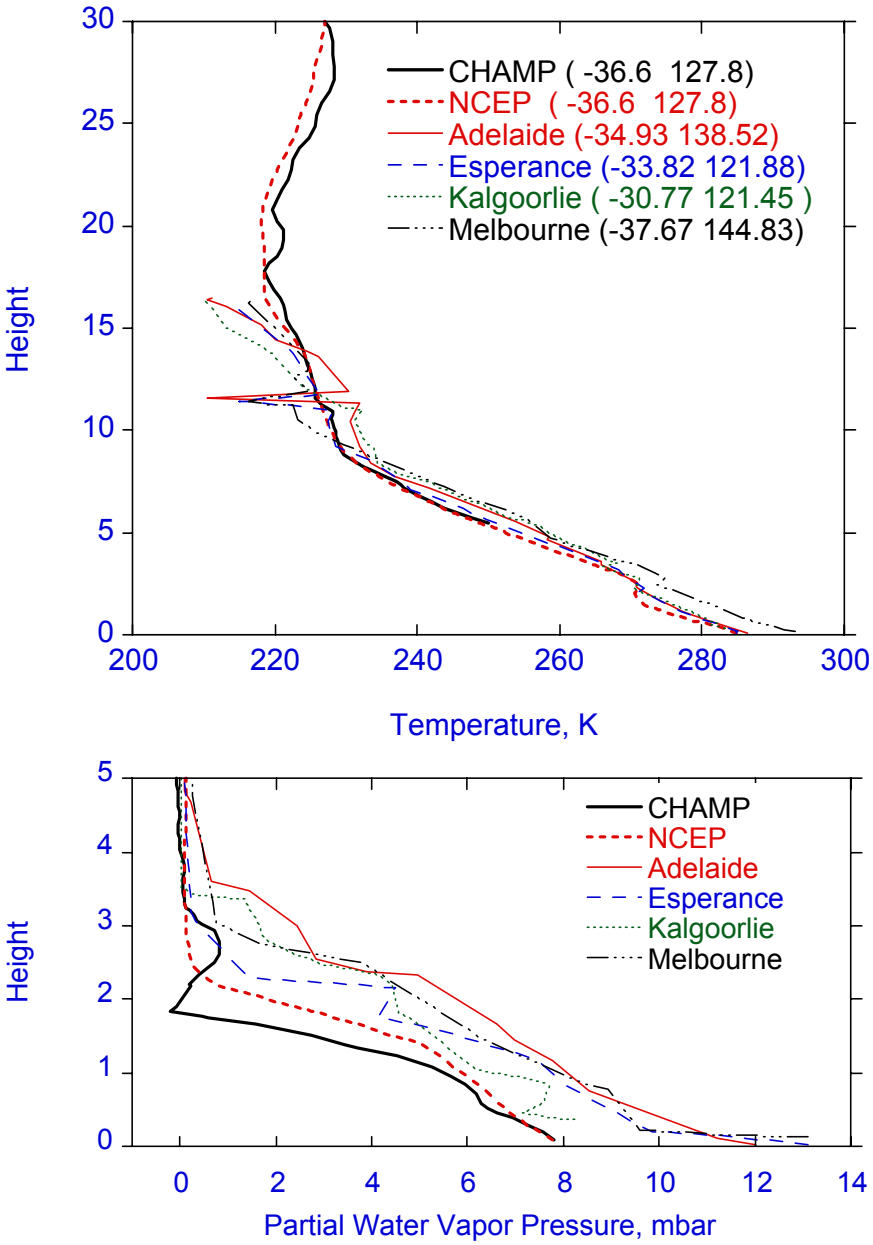

Figure 12. Temperature (top) and water vapor (bottom) of the occultation of figure 11 and corresponding NCEP and nearby rediosonde profiles. CHAMP temperature retrieval is only shown down to the height where T = 250, after which the NCEP temperature is used to derive partial water vapor pressure from CHAMP refractivity.

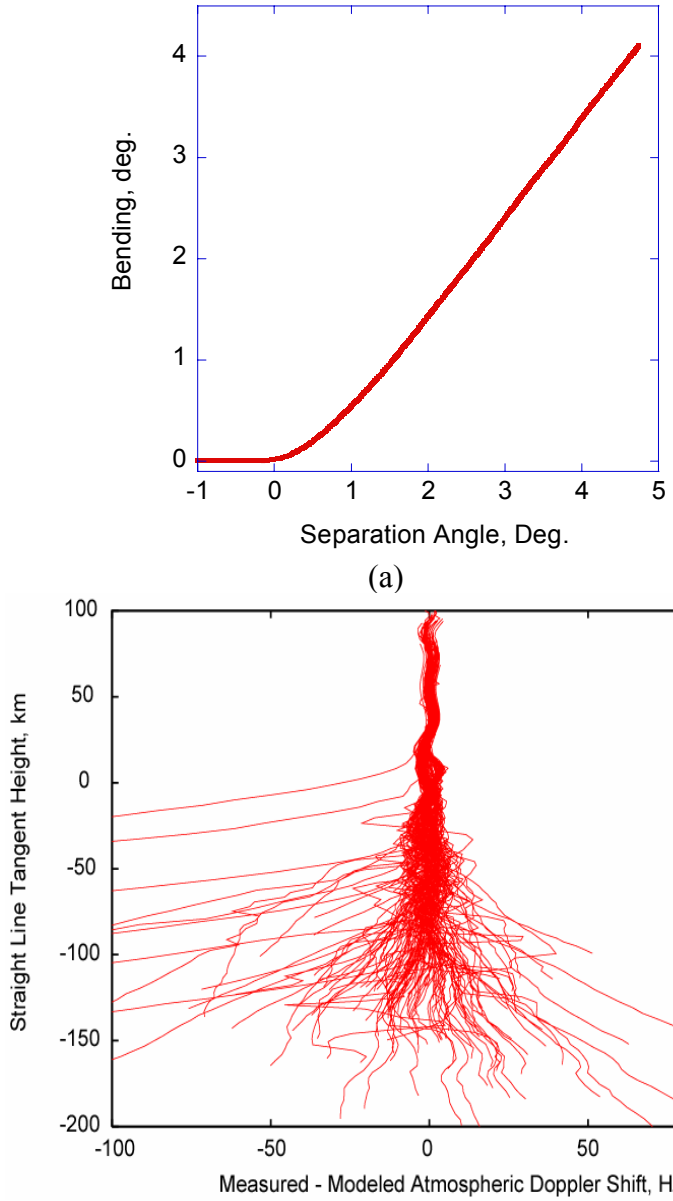

Figure 13: (a) Atmospheric bending as function of separation angle between the transmitter and the receiver showing the strong linear relationship between them in the troposphere which can be exploited to derive a model for the Doppler shift of the occulted signal independent of any atmospheric model. (b) The difference between the measured and modeled Doppler shift for all SAC-C occultations collected in one day at the 100 Hz rate. The Doppler shift model is based on Figure 13.a. Deviations larger than ±50 Hz are indicative of episodes where the receiver is not tracking properly.

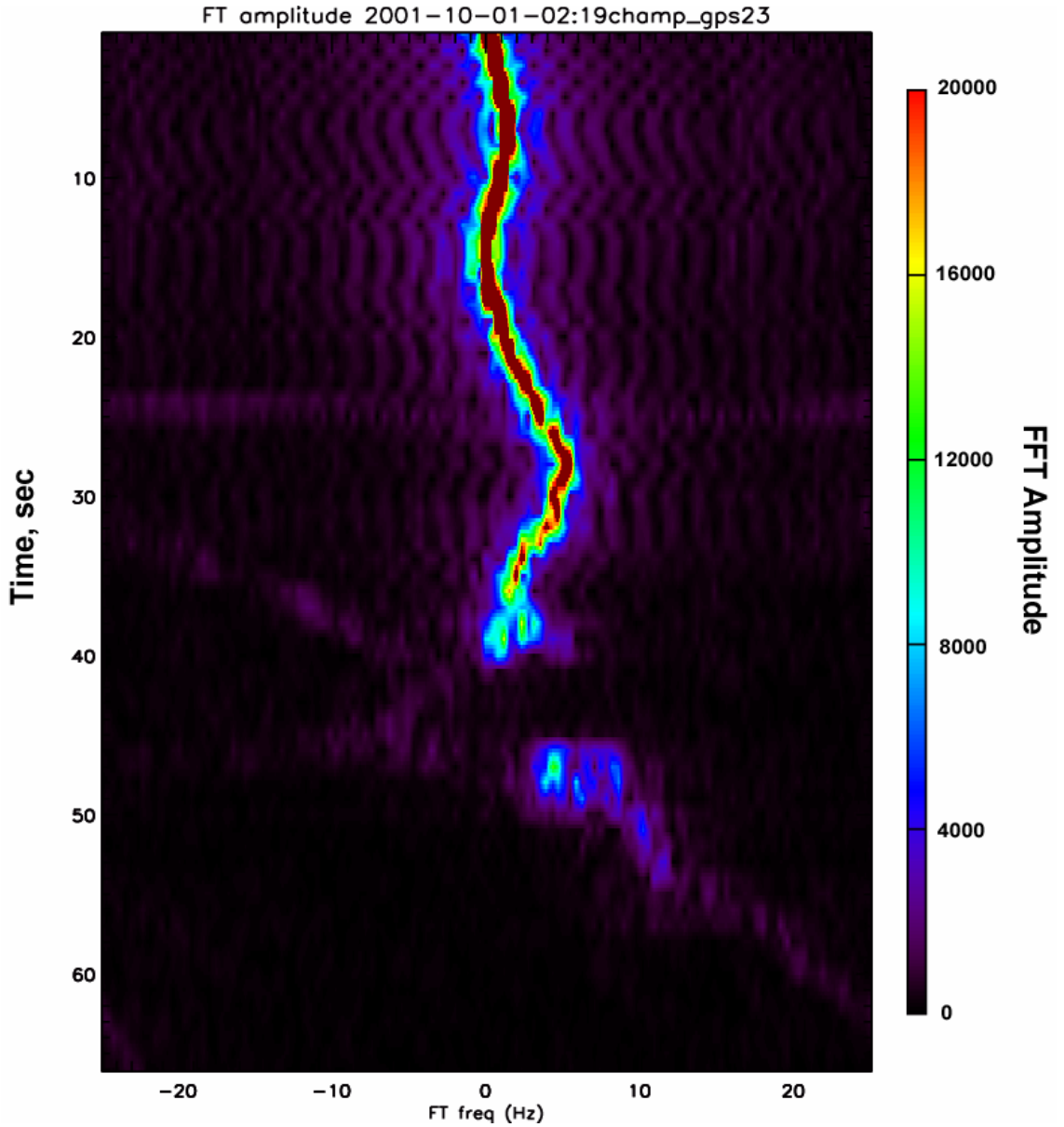

Figure 14. Fast Fourier transform of the complex (real and imaginary) difference between the received and modeled signal of the occultation in Figure 11. The FFT is computed based on a 2-second moving window. Immediately before and after the signal gap (between 38-48 seconds), multiples tones can be seen as evidence of atmospheric multipath. The signal running diagonally starting at ~30 sec. corresponds occulted signal reflected off the ocean's surface.

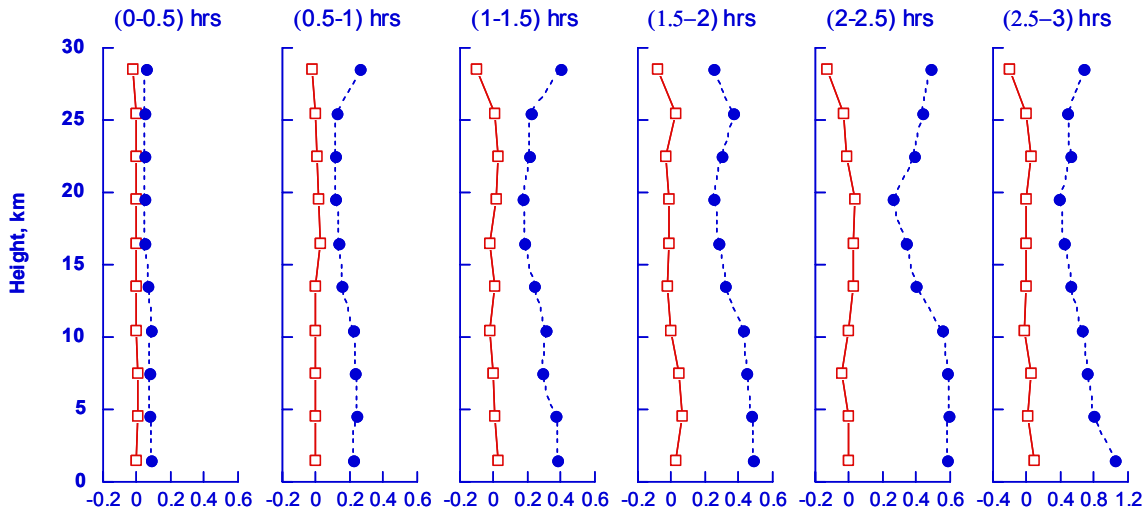

Figure 15: Mean (squares) and standard deviation (circles) of temperature differences (in degrees) as a function of height between two sets of profiles: (1) NCEP temperature at CHAMP occultation location and time and (2) NCEP temperature at CHAMP occultation location and SAC-C occultation time. The statistics are binned according to the time separation between CHAMP and SAC-C to provide a measure of temporal variation of the atmosphere according to the NCEP analysis.

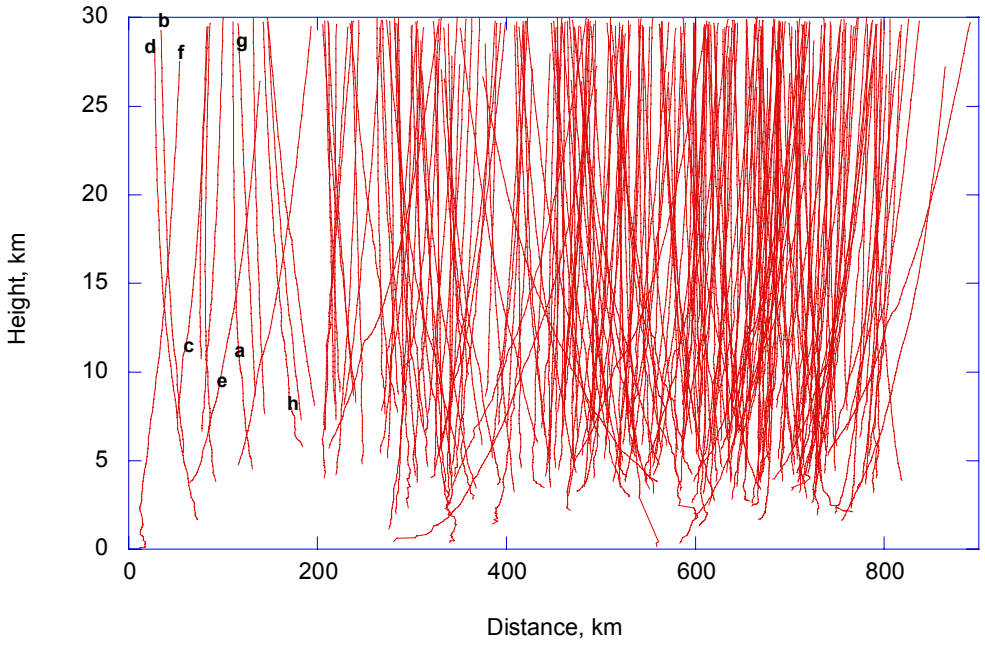

Figure 16: Each line corresponds to a CHAMP-SAC/C pair of occultations that are <0.5 hrs and < 800 km apart and shows the distance between tangent points as a function height. All occultations from the period Aug. 22, 2001 to Oct. 15, 2001 satisfying the condition above are shown. Marked a-h are the nearest pairs shown in Figure 18.

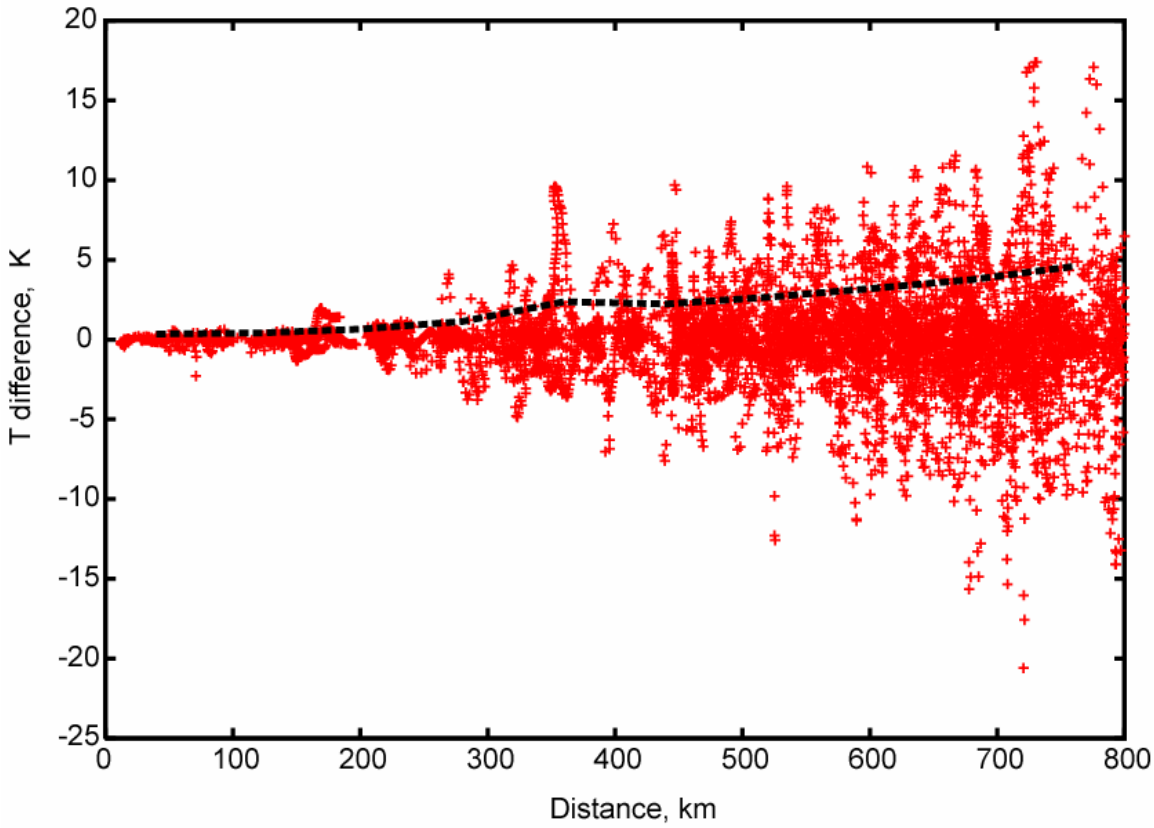

Figure 17: Temperature difference as a function of distance between pairs of NCEP profiles obtained at the coincident occultations of Figure 16. The RMS difference is indicated by the solid dashed line.

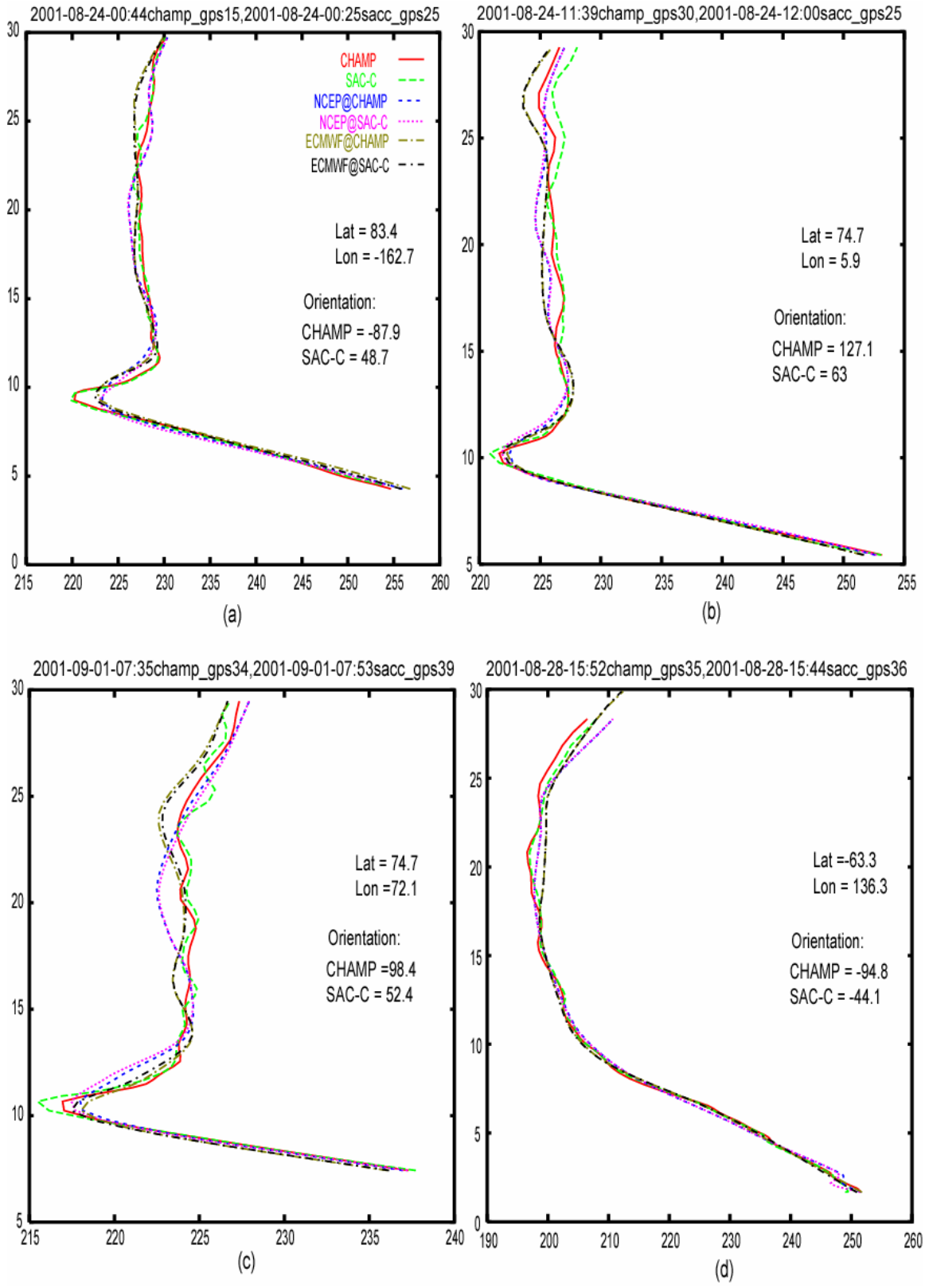
2001-08-24-00:44champ_gps15,2001-08-24-00:25sacc_gps25
CHAMP
SAC-C
NCEP@CHAMP
NCEP@SAC-C
ECMWF@CHAMP
ECMWF@SAC-C
Lat = 83.4
Lon = -162.7
Orientation:
CHAMP = -87.9
SAC-C = 48.7
(a)
2001-08-24-11:39champ_gps30,2001-08-24-12:00sacc_gps25
Lat = 74.7
Lon = 5.9
Orientation:
CHAMP = 127.1
SAC-C = 63
(b)
2001-09-01-07:35champ_gps34,2001-09-01-07:53sacc_gps39
Lat = 74.7
Lon =72.1
Orientation:
CHAMP =98.4
SAC-C = 52.4
(c)
2001-08-28-15:52champ_gps35,2001-08-28-15:44sacc_gps36
Lat =-63.3
Lon = 136.3
Orientation:
CHAMP = -94.8
SAC-C = -44.1
(d)

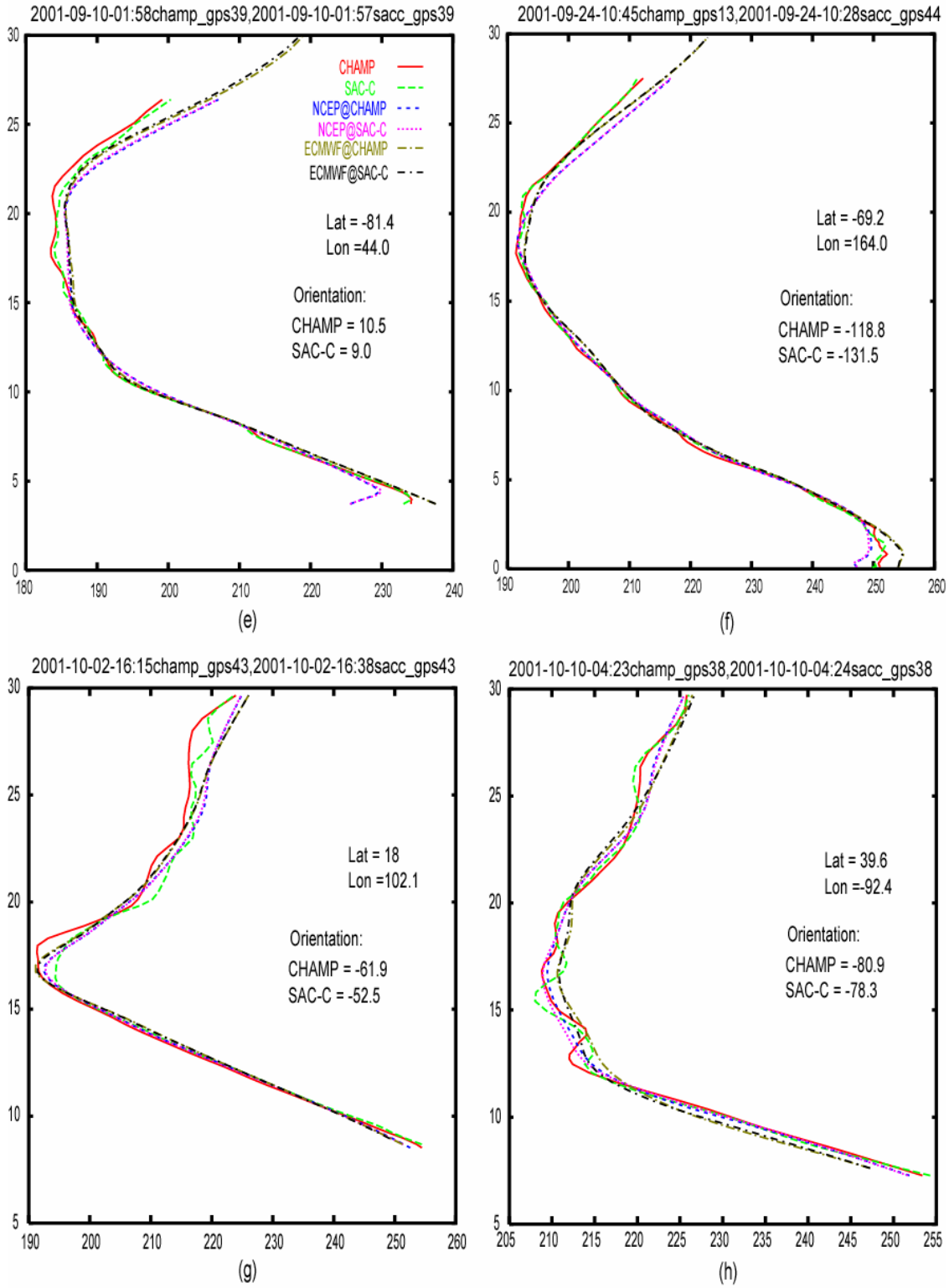

Figure 18: Examples of CHAMP and SAC-C occultations that are < 1/2 hrs. and < 200 km apart for the period Aug. 22, 2001 to Oct. 15, 2001. The labels a-h correspond to those of figure 16. Also shown are NCEP and ECMWF analyses at the CHAMP and NCEP locations and times, the average latitudes and longitudes of the occultations, the orientations of CHAMP and SAC-C occultation links (measured in degrees counterclockwise from East), and the IDs of the pair of occultations compared (each ID indicates the date, hours, minutes and two satellites, e.g., CHAMP and GPS15, that are being occulted).

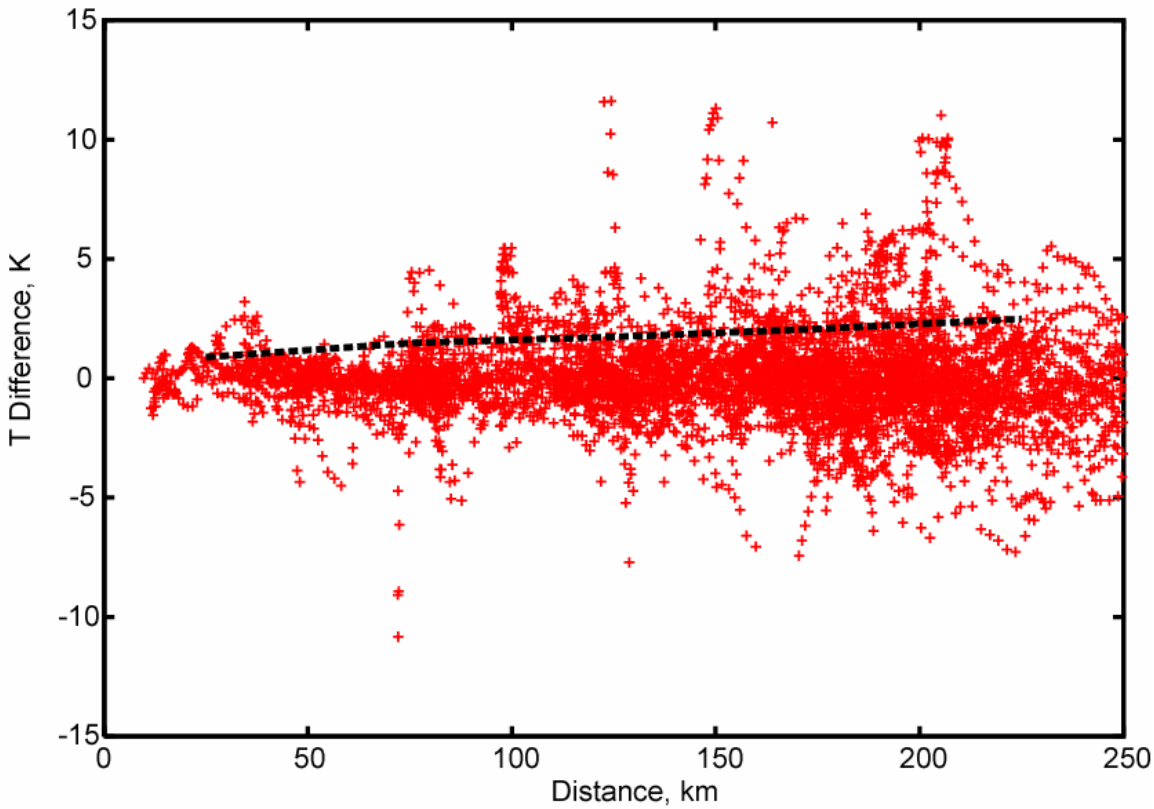

Figure 19: Temperature difference as a function of distance between pairs of CHAMP and SAC-C occultations that are < ½ apart. The RMS difference is indicated by the solid dashed line.

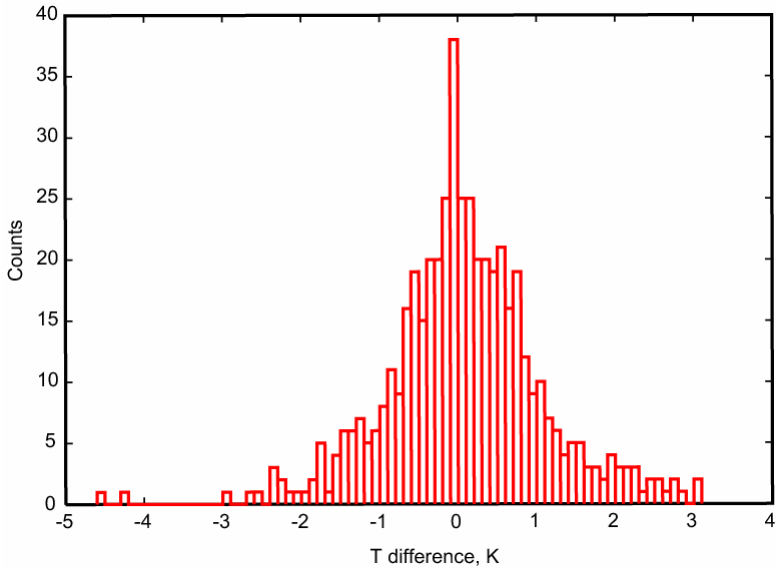

Figure 20: A histogram of CHAMP and SAC-C temperature differences for all points in occultation pairs that are between 5-10 km altitude and within 150 km from each other.

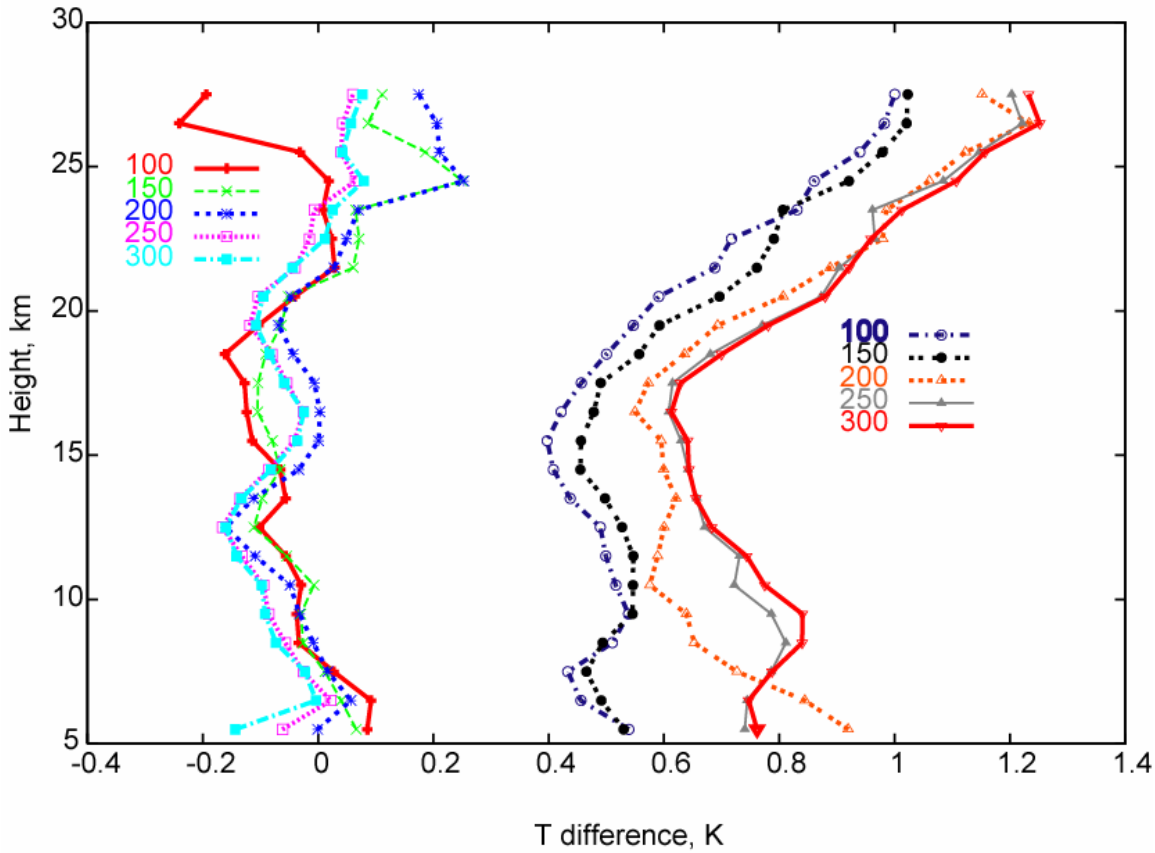

Figure 21: Median (left set of curves) and 68% confidence interval (right set) of temperature differences between CHAMP and SAC-C as a function of height for measurements < (100, 150, …, 300) km apart.

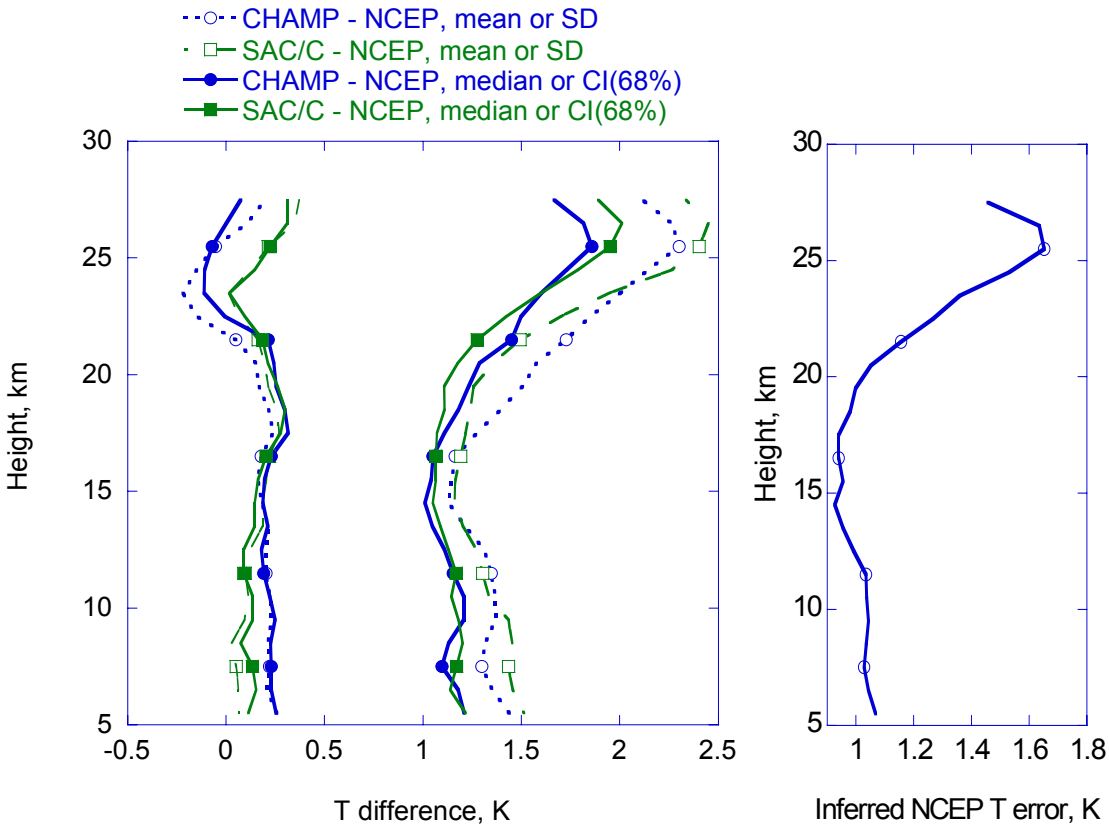

Figure 22: (Left panel) Mean or median (curves clustered around 0) and standard deviation (SD) and 68% confidence interval (CI) of CHAMP – NCEP and SAC/C – NCEP temperatures for the 60 coincident CHAMP and SAC/C pairs. (Right panel) Inferred temperature error (1-σ) of the NCEP analysis.

Table 1. Residual of SLR measurements to CHAMP.

Day	Data points	RMS (m)	Std (m)
152	49	0.020	0.016
153	133	0.058	0.027
154	59	0.058	0.033
155	54	0.109	0.023
156	85	0.107	0.107
157	59	0.084	0.073
158	114	0.072	0.062
159	53	0.023	0.020
160	25	0.056	0.040